Redistribution of the soil ^{137}Cs inventory through litter and sediment transport on a hillslope covered by deciduous forest in Fukushima, Japan

Authors

Tomoki Oda[1, 2*], Norifumi Hotta[2], Satoru, Miura[1], Izuki Endo[3], Keitaro Tanoi[2], Chris S. Renschler[4], Nobuhito Ohte[5]

1. Department of Disaster Prevention, Meteorology and Hydrology, Forestry and Forest Products Research Institute, Ibaraki 305-8687, Japan

2. Graduate School of Agricultural and Life Sciences, The University of Tokyo, 1-1-1 Yayoi, Bunkyo-ku, Tokyo 113-8657, Japan

3. School of Human Science and Environment, University of Hyogo, Hyogo 670-0092, Japan

4. Department of Geography, University at Buffalo, The State University of New York, 116 Wilkeson Quad, Buffalo NY 14261, USA

5. Department of Social Informatics Graduate School of Informatics, Kyoto University, Kyoto 606-8501, Japan

*Corresponding author: Tomoki Oda

e-mail: tomokioda@affrc.go.jp

Abstract

The long-term behavior of radiocesium (^{137}Cs) activity concentrations in forest ecosystems and their downstream impacts remain important issues in the deciduous broadleaf forests of Fukushima, Japan following the Fukushima Daiichi Nuclear Power Plant accident. To predict ^{137}Cs cycling and discharge in the forest ecosystem, it is important to understand the spatial dynamics of the ^{137}Cs inventory and transport along hillslopes. Therefore, we observed the spatial distribution of the ^{137}Cs inventory and ^{137}Cs transport via sediment and litter of a deciduous forest hillslope in Fukushima, Japan in 2016 and 2017 and examined how the spatial distribution of ^{137}Cs inventory was formed using a mass balance model. In 2017, the ^{137}Cs activity concentration was significantly greater in the downslope riparian area (455 kBq/m^2) than in the upslope ridge area (179 kBq/m^2). Annual ^{137}Cs transport within litter and sediment contributed < 0.5% to the current ^{137}Cs inventory, and cannot explain the current spatial variation of ^{137}Cs inventory on the hillslope. The mass balance model results showed that if the initial ^{137}Cs deposition was distributed uniformly in 2011, the spatial distribution of the hillslope ^{137}Cs inventory was influenced mainly by the movement of leaf litter with a high ^{137}Cs activity concentration.

Keywords: ^{137}Cs inventory, Forest hillslope, Deciduous forest, Litter transport, Soil erosion

1. Introduction

The March 2011 accident at the Fukushima Daiichi Nuclear Power Plant (FDNPP) led to the release of a large amount of radioactive material and fallout over a forested area covering approximately 70% of Fukushima Prefecture, Japan. One of the radioactive materials released, radiocesium (^{137}Cs), has a long half-life of approximately 30 years and therefore has long-term effects on ecosystems including forests. Studies have illustrated that ^{137}Cs was either directly deposited on the forest floor or transported via throughfall, stemflow, or litterfall (Kato et al., 2017, 2019a). Most ^{137}Cs in the forest floor was adsorbed onto the soil surface within the uppermost 10 cm of soil (Nakanishi et al., 2014; Takahashi et al., 2015, 2018); some of this ^{137}Cs was incorporated into ecosystem cycles (Hashimoto et al., 2012; Murakami et al., 2014; Imamura et al., 2017), and less than 1–2% of the total deposited ^{137}Cs flowed out of forested watersheds (Iwagami et al 2019; Taniguchi et al., 2019; Nakanishi et al., 2021). Because most ^{137}Cs remained in the forest, the determination of its spatial and temporal dynamics, its long-term runoff and sedimentation redistribution process, and its impacts on ecosystems in general is essential.

According to studies of ^{137}Cs dynamics in forested areas near Chernobyl, Ukraine, the majority of ^{137}Cs released from that accident remained in the organic and mineral soil layers of the forest floor for decades (Shcheglov et al., 2001; Konoplev et al., 2016). The accumulation of ^{137}Cs in the surface soil of the Fukushima-area forests is similar to that around Chernobyl

(Pumpanen et al., 2016; Takahashi et al., 2018). Thus, most of the ^{137}Cs is expected to remain in the surface soil well into the future. However, the climatic and geographic conditions of Fukushima watersheds, which have steep slopes and high precipitation, differ considerably from those of Chernobyl (Konoplev et al., 2016). The geographic and climatic characteristics of forested areas in Japan may result in greater surface transport of ^{137}Cs along hillslopes to valley bottoms via litter movement and soil redistribution. Previous studies have primarily focused on ^{137}Cs transport immediately following the accident, and lateral movement of ^{137}Cs along the forest floor via soil erosion measured in hardwood and cedar forest slope plots accounted for less than 3% of the initial ^{137}Cs deposited (Yoshimura et al., 2015: Niizato et al., 2016; Wakiyama et al., 2019; Onda et al., 2020a). The contribution of leaf litter movement to the redistribution of ^{137}Cs on slopes has been reported (Koarashi et al., 2014; Sakai et al., 2016; Onda et al., 2020b). However, few studies into the effects of ^{137}Cs movement on the spatial and temporal redistribution of ^{137}Cs inventory have been conducted based on the measurement of transported sediment and litter at the hillslope scale.

To understand the process of ^{137}Cs redistribution on a hillslope, it is necessary to consider temporal changes from the ^{137}Cs fallout event to the present. The dominant forest type in the area most strongly affected by the FDNPP accident is deciduous broadleaf forest (49.1% of the total forested area) (Hashimoto et al., 2012). In this deciduous broadleaf forest, most of ^{137}Cs was attached to surface materials on the forest floor at the time of ^{137}Cs deposition in 2011

(Kato et al., 2017; Onda et al., 2020b), and ^{137}Cs activity concentrations in the ground litter and surface soil at the time were likely higher than their current levels. Furthermore, the downslope movement of leaf litter is greater in deciduous broadleaf forests than in coniferous forests (Hart et al., 2013), affecting the material cycles the forest ecosystem (Fisher, 1977; Tsukamoto, 1991; France, 1995; Sakai et al., 2016) as well as erosion on forest slopes (Sala, 1988; Larsen et al., 1999; Wakahara et al., 2008; Ghahramani et al., 2011). In the deciduous forests of Fukushima, December through March is the deciduous season, and at the time of the FDNPP accident, most of the ^{137}Cs was deposited directly on the forest floor without being intercepted by the forest canopy, and the subsequent movement of high contaminated litter and surface soil along the hillslope might have led to significant redistribution of ^{137}Cs along the forested hillslope.

The objective of this study was to clarify the spatial variation of ^{137}Cs inventory in the forest hillslope and examine the influence of lateral movements of sediment and litter down a slope on the temporal and spatial distributions of the soil ^{137}Cs inventory in a deciduous forest. We established a hillslope plot extending from a ridge to the adjacent valley bottom on a steep slope covered with deciduous forest and measured the spatial distribution of soil ^{137}Cs as well as ^{137}Cs transport through lateral movements of sediment and litter. Then, we evaluated the origin of spatial variations in the ^{137}Cs inventory on the slope and assessed the effects of lateral transport on ^{137}Cs inventory fluctuations through inverse analysis using a mass balance model.

2. Methods

2.1 Study site

This study was conducted in the forested watershed of the upper Kami-Oguni River in Ryozencho, Date, Fukushima Prefecture, Japan (37°43' N, 140°34' E) (Figure 1a), about 50 km northwest of the Fukushima Daiichi Nuclear Power Plant (FDNPP). The initial deposition of ^{137}Cs in this region was 236 kBq/m^2 (Kato et al., 2019b). From 1981 to 2019, the annual mean precipitation was 1,322 mm and the annual mean temperature was 10.1°C (Japan Meteorological Agency).

We set up a hillslope plot (20 m × 54 m) extending from the riparian zone to the ridge (Figures 1b, 2a). This slope plot was set up in 2012 to quantify ^{137}Cs input into the forest and cycles between trees, and information on litterfall and trees has been accumulated (Endo et al., 2015). The altitude along the uniform hillslope slope ranged from 351 to 390 m and the mean slope angle was 32.7°. This area is covered by deciduous trees, mainly consisting of oaks (*Quercus* spp.) and maples (*Acer* spp.), with a stem density of 1,300 stems/ha.

2.2 Observations

2.2.1. Soil sampling

Soil samples excluding leaf litter were collected at 30 points along the hillslope using a 5.5-cm-diameter soil core sampler (DIK-110C, Daiki Rika Kogyo, Japan) to a depth of 30 cm (Figure

1b). The hillslope plot was divided into six subplots: the streamside (Plot 1, 68 m^2), bottom slope (Plot 2, 166 m^2), lower slope (Plot 3, 195 m^2), middle slope (Plot 4, 228 m^2), upper slope (Plot 5, 276 m^2), and ridge (Plot 6, 144 m^2), at intervals of approximately 10 m. Five soil samples were collected in each subplot on November 4, 2017 (Figure 1b, c). Within each plot, soil samples were collected at the same elevation level, but in plot 6, soil samples were collected along the ridge and therefore resulting in a difference in elevation.

2.2.2. Leaf litter and other transported material on the slope surface

To measure the litter fall amount and its ^{137}Cs activity concentration, we installed five funnel-shaped litter traps (opening diameter, 0.5 m^2) on the slope surface (Figure 2b). Litter was collected from the traps every 2–3 months from October 2015 to December 2016. Leaf litter on the ground was collected from the litter layer in Plot 2, Plot 3, Plot 4 and Plot 5 with three replicates in December 2016.

Three sediment traps (ST1, ST2, and ST3; Figure 2c, d) were installed along the hillslope to measure the material and ^{137}Cs transport rates (Figure 1b, c). The structure of each sediment trap (width, 1.0 m; depth, 0.2 m; height, 0.2 m) was similar to that of traps used in previous studies (Ghahramani et al., 2011; Imaizumi et al., 2019), including a vertical wire mesh secured by wooden piles at both sides and at the downslope end. A synthetic sheet was placed within the wire mesh and on the adjacent ground to trap fine soil and litter (Figure 2c, d). Nearly all of the transported material was litter, with fine soil particles attached to the litter. Trapped material was collected at intervals of 1–3 months from September 2016 to March 2018.

2.3 Analyses

2.3.1. Analyses of ^{137}Cs activity concentration in litter, soil, and other transported material

Samples of litter and other transported material were dried in an oven at 60°C for at least 48 h. The soil core samples were divided into 1-cm increments to a depth of 10 cm, 2-cm increments for depths of 10–20 cm, and 5-cm increments for depths of 20–30 cm. After drying, the dry weight of each sample was measured, and the samples were crushed finely and packed into 20-mL polypropylene containers. The ^{137}Cs activity concentration of each sample was measured over 20 min using a well-type NaI(Tl) scintillation automatic gamma counter (2480 WIZARD2, PerkinElmer Japan Co., Ltd., Yokohama, Japan), following the manufacturer's protocol. The ^{137}Cs activity measurement error was within 5% and 10% for the litter and soil samples, respectively. Measurements were corrected for the sampling day.

2.3.2. ^{137}Cs inventory, ^{137}Cs deposition via litterfall, and lateral ^{137}Cs movement on the forest floor

The total ^{137}Cs activity to a depth of 30 cm was assumed to equal the total ^{137}Cs inventory in the soil, as previous studies have demonstrated that negligible ^{137}Cs is present below a depth of

20 cm in the soil of broadleaf forests (Nakanishi et al., 2014; Takahashi et al., 2018). The annual litterfall amounts, LF [kg/m^2/yr], for 2015 and 2016 were calculated as the sums of the average observed litterfall amounts for each observation period from October to December 2015 and from January to December 2016, respectively. The observation period for 2015 was shorter; however, the litterfall amount recorded during the sampling period was treated as the annual litterfall because more than 90% of the annual litter production on the hillslope occurs from October to December (Endo et al., 2015). We calculated the annual volume-weighted ^{137}Cs activity concentration, C_{LF} [kBq/kg], by dividing the annual ^{137}Cs input through litterfall, Q_{LF} [kBq/m^2/yr], by LF.

We calculated the annual material transport rate, TM [kg/m^2/yr], from the annual material transport amount observed from January to December in 2017 [kg/yr] and the contributing area [m^2], defined as the drainage area at each sediment trap location, as determined by topography. We calculated the contributing areas for the sediment traps using a 2-m-mesh digital elevation model and conducted geographic analysis using ArcGIS (ESRI Inc., Redlands, CA, USA). We calculated the annual transport of ^{137}Cs, Q_{TM} [kBq/m^2/yr], from the sediment traps by summing the product of the material transport rate and the ^{137}Cs activity concentration [kBq/kg] for each observation period. The volume-weighted mean ^{137}Cs activity concentration in transported material, C_{TM} [kBq/kg], was calculated from Q_{TM} and TM. To compare the observed C_{TM} and TM values in this study with those obtained in other areas, we calculated the entrainment coefficient, Sc [m^2/kg] (Yoshimura et al., 2015; Wakiyama et al., 2019; Onda et al., 2020a), defined as the ^{137}Cs activity concentration in transported material per unit ^{137}Cs initially deposited. A rainfall erosivity factor, R [MJ mm/ha h] was calculated to evaluate the impact of rainfall intensity on TM. The R for a given period was calculated as follows:

$$R = \sum_{i=1}^{n} E_i I_{30i} \tag{1}$$

where E_i is the energy in rainfall (MJ/ha) and I_{30i} is the maximum half-hour rainfall intensity (mm/h) for a storm (i) (Yoshimura et al., 2015; Wakiyama et al., 2019). In the forest, throughfall intensity differs from open rainfall intensity due to the rainfall partitioning into an interception, a throughfall, and a stemflow component. Previous studies, however, have indicated that the intensity of open rainfall is proportional to the kinetic energy of throughfall including free throughfall, drips, and splash water droplets (Nanko et al., 2008). The stemflow amount is usually much smaller than throughfall (approximately 10% of the throughfall amount) (Endo et al., 2015) and therefore it's effect is considered relatively small. Therefore, the rainfall erosivity factor (R) is an acceptable indicator for erosion in the forest ground.

The transported material consisted of litter and sediment. We calculated the contribution rate of litter to TM, p, using $C_{TM}(t)$; the mean ^{137}Cs activity concentration in the leaf litter, $C_{litter}(t)$, assuming that $C_{litter}(t)$ was similar to $C_{LF}(t)$; and the mean ^{137}Cs activity concentration in the surface soil between depths of 0 to 1 cm, $C_{soil}(t)$ [kBq/kg], as shown below:

$$C_{TM}(t) = p\, C_{litter}(t) + (1 - p)\, C_{soil}(t). \tag{2}$$

The contribution rate of litter transport to Q_{TM}, q, was described using TM and p, as follows:

$$Q_{TM}(t) = (p\ q\ C_{litter}(t) + (1 - p)\ (1 - q)\ C_{Soil}(t))\ TM. \quad (3)$$

2.3.3. Modeling ^{137}Cs transport along the forest floor

We estimated how the initially deposited ^{137}Cs, $S_{initial}$ [kBq/m^2], was redistributed on the hillslope using a mass balance model. Annual changes in the ^{137}Cs inventory, along with Q_{TM} from the ridge to the riparian area, were calculated for the 2011–2017 period. The contour lines in the subplots used in this study were generally parallel, and transported materials were assumed to move orthogonally with respect to the contour lines. The distance of each observation point from the ridge was calculated, and the average contribution area per unit width of each subplot was obtained.

Based on the topography of the slope, the areas around the sampling points in Plots 1 and 2 at the toe slope, where the average slope (12°) was distinctly gentler than at other points (34°), were defined as the deposition area (riparian area). The average distance from the ridge top (averaged location of observation points in Plot 6) to the average location of an observation point in Plot 1 was x_1 [m] (53.9 ± standard deviation: 3.9 m). Additionally, the source slope area (slope area), including Plots 3, 4, and 5, and the source ridge area (ridge area), including Plot 6, were identified. The boundaries between the riparian, slope, and ridge areas were the middle points between Plots 2 and 3 and between Plots 5 and 6, respectively, with the respective distances from the ridge top denoted x_2 [m] (42.2 ± 2.9m) and x_3 [m] (7.2 ± 2.4 m).

Redistribution of the ^{137}Cs inventory was assumed to be driven by lateral transport associated with sediment and litter movement over the ground surface, and fluctuations due to vertical movements in soil layers deeper than 30 cm were assumed to be negligible. The ^{137}Cs inventories of the riparian area, $S_{rip}(t)$, slope area, $S_{slope}(t)$, and ridge area, $S_{ridge}(t)$, over time t since 2011 (measured in years) were determined as shown below:

$$dS_{rip}(t) / dt = x_2 \, Q_{TM}(x_2, t) / (x_1 - x_2), \tag{4}$$

$$dS_{slope}(t) / dt = (x_3 \, Q_{TM}(x_3, t) - x_2 \, Q_{TM}(x_2, t)) / (x_2 - x_3), \tag{5}$$

$$dS_{ridge}(t) / dt = -Q_{TM}(x_3, t). \tag{6}$$

$S_{initial}$ was assumed to have fallen uniformly over the entire area in March 2011, i.e., $S_{initial} = S_{rip}(0) = S_{slope}(0) = S_{ridge}(0)$ for $t = 0$. Previous studies have suggested that the initial level of ^{137}Cs deposition changes with elevation, and that canopy interception affects the initial spatial distribution on the ground (Atarashi-Ando et al., 2015; Schaub *et al.*, 2010). In the Fukushima forest, although a relationship between elevation and air dose rate was found in a 0.6-km^2 watershed with elevations ranging from 588 to 724 m, due to the large air dose rate at the summit, no clear relationship was observed on the slopes with an elevation difference of 30-50 m from the middle ridge to the valley (Atarashi-Ando *et al.*, 2015). In our study site, this effect is assumed to be small because the difference in elevation from the middle ridge to valley was only 40 m (350–390 m), and deciduous broadleaf trees covered nearly the entire slope. $S_{initial}$

was estimated from the current area-weighted average ^{137}Cs inventory because the majority of $S_{initial}$ remained in the forest soil without being exported to streams (Ohte et al., 2016) and the ^{137}Cs inventory in tree trunks and branches was less than 10% (Murakami et al., 2019) in this study area.

The ^{137}Cs inventory at each sampling point was assumed to consist of three inventories: those of leaf litter, $S_{litter}(x_n, t)$; surface soil from 0 to 1 cm, $S_{soil}(x_n, t)$; and subsurface soil below 1 cm, $S_{subsoil}(x_n, t)$ [kBq/m^2] (n = 1, 2, and 3) (Figure 3). All of $S_{initial}$ was assumed to adhere to litter or surface soil, as trees in the deciduous forest lacked leaves at the time of the accident, and therefore, most radionuclides were deposited directly onto the forest floor without canopy interception. The parameter indicating the adhesion rate to litter under initial conditions was denoted α.

$$\alpha\, S_{initial} = S_{litter}(x_n, 0), \tag{7}$$

$$(1 - \alpha)\, S_{initial} = S_{soil}(x_n, 0), \tag{8}$$

$$S_{subsoil}(x_n, 0) = 0, \tag{9}$$

where S_{litter} and S_{soil} contribute to lateral movement, whereas $S_{subsoil}$ is immobile.

$Q_{TM}(x_n, t)$ was determined as follows:

$$Q_{TM}(x_n, t) = C_{litter}(x_n, t) \times p\, TM(x_n, t) + C_{soil}(x_n, t) \times (1 - p)\, TM(x_n, t). \tag{10}$$

The ground litter ^{137}Cs activity concentration at location x and time t, $C_{litter}(x_n, t)$ [kBq/kg], was calculated from the amount of leaf litter on the ground, $LG(x_n, t)$ [kg/m^2], and $S_{litter}(x_n, t)$, as follows:

$$C_{litter}(x_n,\ t) = S_{litter}(x_n\ ,\ t)\ /\ LG(x_n,\ t)\ , \tag{11}$$

where $LG(x_n,\ t)$ was calculated using a constant decomposition rate, β, the litter contribution in $TM(x_n, t)$, p, and LF, as follows:

$$LG(x_n,\ t) = (1 - \beta)\ (LG(x_n,\ t\text{-}1) - p\ (TM(x_n,\ t) - TM(x_{n-1},\ t)) + LF. \tag{12}$$

$LG(x_n,\ t)$ was calculated over 10 years before the initiation time of the model (March 2011), and the converged value was used as the initial value ($LG(x_n, 0)$). $TM(x_n, t)$ was calculated from the relationship between observed TM and the contribution area in 2017 (Figure S3a). $TM(x_n, t)$ for each area was assumed to be similar across all years. The annual precipitation (1222 mm/yr) and maximum daily rainfall (108 mm/day) values from 2017 are comparable to the average annual precipitation ± standard deviation (SD) (1322 ± 244 mm/yr) and maximum rainfall (120 ± 62 mm/day) calculated from rainfall data collected at a nearby weather station since 1981. In this model, TM is assumed to be that of continuous average rainfall. In addition to surface material transport, subsurface pipe flow influences hillslope runoff processes and soil transport by erosion (Jones, 1987). Although cases of subsurface pipe flow have been reported on forest slopes in Japan (Uchida et al., 2001), no case of surface soil-particle transport by subsurface flow has been reported in this area. Therefore, the soil particle transport of the subsurface is considered negligible.

The ^{137}Cs activity concentration in 1-cm-deep surface soil at x_n [m] from the ridge at time t,

$C_{soil}(x_n, t)$, was calculated from $S_{soil}(x_n, t)$ and the soil density, $D = 0.194$ Mg/m^3, measured as the average density of surface soil from 0 to 1 cm, as follows:

$$C_{soil}(x_n, t) = S_{soil}(x_n, t) \,/\, 10D \tag{13}$$

Changes in $S_{litter}(x_n, t)$ and $S_{soil}(x_n, t)$ were calculated using ^{137}Cs transport rates for litter and soil, respectively, as well as vertical ^{137}Cs transfer rates from the litter layer to the soil layer $Q_D(x_n, t)$ [kBq/m^2/yr] and from the surface soil to the subsurface soil, $Q_V(x_n, t)$ [kBq/m^2/yr] (Figure 3), the ^{137}Cs activity concentration in the litterfall, $C_{LF}(t)$, and uptake by plants, Q_{UP} [kBq/m^2/yr], as shown below:

$$dS_{litter}(x_n, t) \,/\, dt = C_{LF}(t) \times LF(t) - p(C_{litter}(x_n, t) \times TM(x_n, t) - C_{litter}(x_{n-1}, t) \times TM(x_{n-1}, t)) - Q_D(x_n, t), \tag{14}$$

$$dS_{soil}(x_n, t) \,/\, dt = Q_D(x_n, t) - (1 - p)(C_{soil}(x_n, t) \times TM(x_n, t) - C_{soil}(x_{n-1}, t) \times TM(x_{n-1}, t) - Q_V(x_n, t) - Q_{UP}(x_n, t), \tag{15}$$

$$Q_D(x_n, t) = \beta\, S_{litter}(x_n, t), \tag{16}$$

$$Q_V(x_n, t) = \gamma_n\, S_{soil}(x_n, t). \tag{17}$$

$$C_{LF}(t) = A_1 e^{-(\lambda_1)t} + A_2 e^{-(\lambda_2)t}, \tag{18}$$

^{137}Cs deposition via litter fall, Q_{LF}, was calculated from $C_{LF}(t)$ along with the average LF (0.4 kg/m^2/yr). $C_{LF}(t)$ was fitted to concentrations observed from October 2012 to September 2013 (Endo et al., 2015) at this study site and data from October 2013 to December 2014 (Endo, unpublished data) using the double exponential model (Kato et al., 2017; Onda et al, 2020b), where A_1 and A_2 denote the initial activity concentration levels of ^{137}Cs in the litterfall declined rapidly and slowly, respectively, and λ_1 and λ_2 represent rate constants for the rapid and slow decline rate ($year^{-1}$) of the activity concentration in litterfall, respectively. In this study, we assumed that uptake by plants was negligible ($Q_{UP}(x_n, t) = 0$) for the entire period, as the amount taken up by plants was less than 1% of the soil ^{137}Cs inventory (Plamboeck et al., 2000; Imamura et al., 2021).

In this study, the annual ^{137}Cs transfer ratio between the litter and soil due to decomposition, β [1/yr], was set to 0.7, as Endo et al. (2018) reported a decomposition rate of 0.6 to 0.75 and Nakanishi et al. (2014) reported a decomposition rate of 0.5 to 0.8 according to the annual ^{137}Cs leaching rate from litter. The ^{137}Cs transfer ratio due to leaching from the surface soil to the subsurface soil at each area, γ_n, was assumed to be constant among years. γ_n was fitted to the calculated ratio of $S_{soil}(x_n, t)$ to the ^{137}Cs inventory of each area and was similar to the average observed ratio of ^{137}Cs accumulated in the 1-cm surface layer to the ^{137}Cs inventory in 2017. The parameter values for the model and their symbols are listed in Table 1.

3. Results

3.1 Soil ^{137}Cs activity concentration and inventory

The profiles of ^{137}Cs activity concentration in each soil sampling subplot in November 2017 are shown in Figure S1, respectively. We found that the ^{137}Cs activity concentration was highest within 5 cm of the surface soil layer with high organic matter content and decreased with increasing depth. At depths of > 20 cm, ^{137}Cs activity concentrations were < 0.1 kBq/kg in all subplots. The mean ^{137}Cs activity concentration in leaf litter on the ground (C_{litter}) in December 2016 was 0.96 ± 0.47 kBq/kg. The C_{litter} was lower than the ^{137}Cs activity concentration of surface soil layer (12-54 kBq/kg) (Figure S1).

The ^{137}Cs inventories of each subplot are shown in Figure 4. The mean ± standard deviation (SD) ratios of soil surface (depth, 1 cm) to total (across the entire soil depth sampled) ^{137}Cs activity concentration for the riparian, slope, and ridge subplots were 13 ± 11%, 20 ± 13%, and 20 ± 10%, respectively. Greater surface soil ^{137}Cs accumulation was observed in slope and ridge areas than in riparian areas.

The relationship of the average distance between each subplot and the stream channel with the average soil ^{137}Cs inventory of the subplots is shown in Figure 5. The mean ± SD ^{137}Cs inventory within the study area was 322 ± 227 kBq/m^2. The area-weighted average ^{137}Cs inventory was 294 kBq/m^2. The average ^{137}Cs inventory of the riparian (subplots 1 and 2), slope (subplots 3, 4, and 5), and ridge (subplot 6) areas were 455 ± 287, 269 ± 173, and 212 ± 113 kBq/m^2, respectively.

3.2 ^{137}Cs deposition via litter

The litter amounts collected in 2015 and 2016 were 0.32 ± 0.03 and 0.50 ± 0.06 kg/m^2/year, respectively. The annual ^{137}Cs deposition rates via litterfall (Q_{LF}) in 2015 and 2016 were 0.15 ± 0.04 and 0.35 ± 0.08 kBq/m^2/year, respectively. The volume-weighted mean ^{137}Cs activity concentration in litter (C_{LF}) from 2015 to 2016 was 0.62 kBq/kg. Comparing our data to those reported in previous studies for the same site (2012–2013, Endo et al., 2015; 2014, Endo, unpublished data), $C_{\mathrm{LF}}(t)$ declined rapidly in the two years following initial fallout and has declined moderately in years 3 to 6 (Figure S2).

3.3 Lateral transport of ^{137}Cs

The *TM* values of ST1, ST2, and ST3 were 0.027, 0.088, and 0.2 kg/m^2/yr, respectively, and Q_{TM} values for the transport of ^{137}Cs were 0.072, 0.082, and 0.53 kBq/m^2/yr, respectively, from January to December of 2017. *TM* had a negative relationship with the contribution area and a positive relationship with the slope angle (degree) at a given observation point (Figure S3).

The C_{TM} values at ST1, ST2, and ST3 were 2.1, 0.92, and 2.0 kBq/kg, respectively, and the overall average was 1.7 ± 0.89 kBq/kg, which was higher than the ^{137}Cs activity concentration in litterfall (0.62 ± 0.11 kBq/kg) and lower than the average ^{137}Cs activity concentration in 1-cm surface soil (24 ± 21 kBq/kg) (Figure 6). The average *Sc* in 2017 was 0.0051 m^2/kg.

The mean litter contribution rates (*p*) to *TM* at ST1, ST2, and ST3, which were calculated using Eq. (1), were 0.95, 0.99, and 0.96, respectively. The mean contributions of transported litter to Q_{TM} (*q*) at ST1, ST2, and ST3 were 0.3, 0.69, and 0.28, respectively. These results indicate that litter was the main material transported along the hillslope and that ^{137}Cs was transported primarily by soil during the observation period in 2017. The estimated annual ratios of litter transport to litterfall (*pTM*/*LF*) at ST1, ST2, and ST3 were 6.2%, 21%, and 47%, respectively, with an average of 24%. Most *LF* stayed in place on the hillslope; however, spatial variations were observed, with greater movement of litter in the upper slope area.

Seasonal fluctuations in the material transport rate (kg/m^2) varied among observation periods. The daily mean material transport rate was lower during the growing season (April to September; 0.21 ± 0.13 g/m^2/day) than during the dormant season (October to March; 0.33 ± 0.50 g/m^2/day; Figure 7c). No clear correspondence was found between the daily material transport rate and rainfall erosivity factor, *R* (Figure 7a,b, c). The daily mean ^{137}Cs transport rate was markedly higher during the growing season (0.88 ± 1.1 kBq/m^2/day) than during the dormant season (0.37 ± 0.6 Bq/m^2/day; Figure 7d). C_{TM} was higher during the growing season (4.0 ± 2.9 kBq/kg) than during the dormant season (0.8 ± 0.4 kBq/kg; Figure 7e). The contribution rate of litter transport to *TM* (*p*) during the growing season was 0.83, which was lower than the value (0.99) during the dormant season. The mean contribution of transported litter to Q_{TM} (*q*) was 0.77 in the dormant season and 0.13 in the growing season.

3.4 Estimated changes in the ^{137}Cs inventory due to litter and soil transport

Estimated changes in the ^{137}Cs inventory in the riparian zone (S_{rip}), slope (S_{slope}), and ridge

(S_{ridge}) from 2011 to 2017 were associated with α values of 0, 0.5, and 1 and are shown in Figure 8. $S_{initial}$ was estimated as 338 ± 167 kBq/m^2. S_{rip}, S_{slope}, and S_{ridge} in 2017 were close to the observed values when α was between 0.5 and 0.8. Conversely, when all of the initially deposited ^{137}Cs adhered to the surface soil (α = 0), the calculated S_{rip}, S_{slope}, and S_{ridge} values varied little from 2011 to 2017 and did not reproduce the observed spatial distribution of the ^{137}Cs inventory (Figure 8). The calculated changes in Q_{TM} values between the ridge and slope area and between the slope and riparian area from 2011 to 2017 (Figure S4) showed that higher α values led to higher Q_{TM} from 2011 to 2012; however, Q_{TM} decreased over time and approached the observed values in 2017 regardless of the value of α. This result indicated that C_{litter} decreased rapidly as litter decomposed over a few years, and the contribution of litter transport to ^{137}Cs movement down the slope decreased with time. The calculated value of Sc was 0.89 m^2/kg in 2011–2012 and converged to the observed Sc in 2017, when α was 0.5. When the initially deposited ^{137}Cs adhered to soil (α = 0), Sc was in the range of 0.005–0.02 m^2/kg during the 2011–2017 period. Calculated LG at ridge and slope were 0.5, 0.6 kg/m^2, respectively.

Sensitivity analysis indicated that the changes in calculated S_{rip} were most sensitive to α and also responded to TM and LG at the time of the accident (Figure S6). These results indicate that, even with some uncertainty, the initial movement of litter with high ^{137}Cs activity concentrations was the most important factor controlling the spatial distribution of the ^{137}Cs inventory on the hillslope.

4. Discussion

4.1 Observed ^{137}Cs inventory on the hillslope

More than 90% of the ^{137}Cs inventory was concentrated in the top 10 cm of surface soil across the entire hillslope (Figure 4); this finding is consistent with previous reports that ^{137}Cs is concentrated at depths of less than 10 cm (Nakanishi *et al*., 2014; Takahashi *et al*., 2015, 2018). The estimated amount of ^{137}Cs initially deposited based on the observed average ^{137}Cs inventory (338 kBq/m^2) exceeded the value (236 kBq/m^2) estimated from the initial ^{137}Cs deposition map constructed by Kato *et al*. (2019b). The initial deposition estimates had uncertainties due to measurement error in aircraft-based inventory estimates for mountainous areas. Field measurements are necessary to estimate ^{137}Cs inventory on a small scale in steep terrain.

The larger ^{137}Cs inventory observed in downslope areas in this study (Figure 5) differed from the reported pattern of a higher air dose rate at higher elevation on a forested hillslope (Atarashi-Ando *et al*., 2015; Schaub *et al*., 2010). Previous studies have suggested that the differences in the spatial distribution pattern of air dose rate were mainly due to differences in initial deposition, and the initial level of ^{137}Cs deposition tends to increase with elevation, and that vegetation type affects the initial spatial distribution on the ground (Atarashi-Ando *et al*., 2015; Schaub *et al*., 2010). Thus, our study site might have received greater initial ^{137}Cs deposition in areas at higher elevation, but the results of the spatial variation of ^{137}Cs inventory, which is greater at lower elevations, obtained in this study are indicated that the initially deposited ^{137}Cs was redistributed across the hillslope via lateral transport of material.

4.2 Observed *LF*, *TM*, and Q_{TM} on the hillslope

The ^{137}Cs activity concentration due to litterfall, C_{LF}, decreased rapidly in the early two years after the accident and was stable from 2013 to 2016 (Figure S2). A decreasing trend in ^{137}Cs input from litterfall was also observed at other sites (Kato *et al*., 2019a). For deciduous broadleaf trees, the reported ^{137}Cs input through litterfall was 10–15% of the total amount deposited, most of which fell to the forest floor within the first year (Kato *et al*., 2017). In this study, the total Q_{LF} after 2012 was less than 2% of the initial ^{137}Cs inventory, and less than 10% of the ^{137}Cs inventory was stored in aboveground vegetation in 2012 (Murakami *et al*., 2019). Therefore, nearly all ^{137}Cs deposited was estimated to have reached the ground in 2011. The remaining ^{137}Cs intercepted by the canopy and absorbed by plants would then supplied to the forest floor by litterfall over a longer time period.

The *TM* (0.03–0.2 kg/m^2/yr) observed in 2017 was similar to the *TM* (0.033–0.13 kg/m^2/yr) observed on the same slope in 2014 (Kashihara et al., 2014) and values reported for Japanese hillslopes with similar slope angles (13–39°) covered with broadleaf forests, with values of 0.004-0.019 kg/m^2 in half a year (Niizato *et al*., 2016), 0.047–0.1 kg/m^2/yr (Nishikiori *et al*., 2015b), and 0.1-1.1 kg/m^2/yr in understory covered plot (Wakahara *et al*., 2008) reported. The relationship between slope angle and *TM* in these previous studies shows an exponential regression line similar to that of the present study (Figure S3), indicating that it is reasonable that the *TM* increases exponentially with increasing slope.

In this study, the average litter transport ratio to *TM* (*p*), estimated using ^{137}Cs as a tracer, exceeded 0.95. This high litter content was consistent with the fact that few trapped sediments were observed and primarily fine particles were attached to the litter. The average amount of litter transported was 24% of *LF*, consistent with reported values ranging from 10% to 30% (Benfield, 1997; Hart *et al*., 2013). In addition, this litter transport is more likely to occur during the dormant season, when little rainfall occurs, suggesting that litter movement is influenced not only by rain but also by wind. The movement characteristics of litter on forest hillslopes have been reported to be basically down-slope movement (Orndorff and Lang, 1981), and the main factors affecting litter movement are understory vegetation, topography, and wind speed (Orndorff and Lang, 1981; France, 1995; Abe et al., 2009). The rate of litter movement on slopes has been measured on forest slopes in Japan with similar tree species, and litter movement has been reported to be approximately 0.1 m/day during the dormant season (Abe et al., 2009) and more active in the dry season of winter and spring than in the wet season of the growing season (Funada et al., 2007; Abe et al., 2009). As for soil movement, it is generally known that surface flow rarely occurs, and raindrop erosion is the main process influencing forest soil movement in Japan (Miura et al., 2002). Therefore, litter movement is larger than soil movement by erosion, which is consistent with the results of this study.

The ^{137}Cs transport rate (Q_{TM}) in 2017 ranged from 0.07 to 0.50 kBq/m^2/yr depending on the slope location. These amounts are 0.02–0.15% of the concurrent ^{137}Cs inventory and are similar to ratios of 0.07–0.2% representing lateral ^{137}Cs transport due to soil wash-off from 2011 to 2014, which were reported in previous studies of the ^{137}Cs inventory on hillslopes covered with coniferous and broadleaf trees (Yoshimura *et al*., 2015; Niizato *et al*., 2016; Wakiyama *et al*., 2019; Onda *et al*., 2020a). The average *Sc* in 2017 was 0.005 m^2/kg, comparable to *Sc* values of 0.003–0.064 m^2/kg for other Japanese forests in 2012–2015 (Onda *et al*., 2020b).

The seasonal change in the ^{137}Cs material transport rate (Figure 7) showed that C_{TM} was higher during the growing season than during the dormant season due to increased sediment transport, and that the litter contribution to transported material, *p*, was lower during the growing season. The climate of the study area makes splash soil erosion more likely in the growing season, when more than 75% of the annual rainfall occurs (Japan Meteorological Agency, 2011–2019), and decreases in litter cover on the ground from fall to spring and summer have been observed (Miura *et al*., 2015). These results indicate that hillslope litter cover and transport are important drivers of temporal variations in ^{137}Cs transport on the hillslope.

4.3 Effects of ^{137}Cs transport on the spatial distribution of ^{137}Cs on the hillslope

In 2017, a higher ^{137}Cs inventory was measured in the riparian area than in the ridge area. The ^{137}Cs mass balance model indicated that current spatial variations in the ^{137}Cs inventory on the hillslope could not be reproduced without ^{137}Cs transport in litter in 2011 and 2012, when the initially deposited ^{137}Cs was distributed uniformly and more than 50% of the initial ^{137}Cs was attached to leaf litter on the ground. The result that no significant change in spatial variation in the ^{137}Cs inventory on the hillslope when the rate of adhesion to the initial litter was 0% ($\alpha = 0$), supported the importance of litter movement on redistribution of ^{137}Cs. These results are consistent with previous findings that lateral transport of leaf litter led to ^{137}Cs accumulation at the bottom of a hillslope (Koarashi *et al*., 2014; Sakai *et al*., 2016; Onda *et al*., 2020b).

In this study, the estimated *Sc* for 2011–2012 was orders of magnitude higher when litter transport was included ($\alpha > 0.5$) than when only sediment transport was considered ($\alpha = 0$) (Figure S5). For sediment transport, the estimated *Sc* from 2012 to 2015 was similar to the range of results in previous studies (Wakiyama *et al*., 2019; Onda *et al*., 2020b). According to Onda *et al*. (2020b), *Sc* in forests in Fukushima gradually trended downward in 2012–2015, and ^{137}Cs transport on sediment had no significant effect on the ^{137}Cs inventory. However, this study showed that early litter migration in 2011 and 2012 could transport a large amount of ^{137}Cs.

In the model, the assumptions that most ^{137}Cs reached the forest floor in 2011 and that more than half of the deposited ^{137}Cs adhered to litter on the forest floor appear reasonable, as the canopy was defoliated and the forest floor covered with litter in March. At the same site, Murakami *et al*. (2014) reported a ^{137}Cs activity concentration greater than 100 kBq/kg in leaf litter on the ground of bottom slope area in 2012, indicating that leaf litter on the ground had a high ^{137}Cs activity concentration similar to the value of C_{litter} calculated in 2012 with an α = 0.5. Hashimoto *et al*. (2020) reported that the contribution of the ^{137}Cs inventory in the mineral soil layer in 2011 was about 50% of the total inventory of the broadleaf forest; the α value (0.5) used here is consistent with their results. Simulated *LG* at ridge and slope areas were 0.5 and 0.6 kg/m^2, respectively. The simulated *LG* values were comparable to the observed values in previous study in forest slope of the same tree species and similar topography (35-40°), which reported that litter abundance was 0.26 – 0.58 kg/m^2 (Koarashi et al., 2014).

The model developed in this study is limited by its simple framework and uncertainties related to measurement error and assumptions about the scales of ridge, slope, and riparian areas, as well as the lateral and vertical ^{137}Cs transport processes. Uncertainties were included in the scales of the ridge, slope, and riparian areas, but the effect of these variations on the calculated ^{137}Cs inventory for each area was less than 5%. This model also assumes that the top 0–1 cm of the surface soil contributes to *TM,* that ^{137}Cs is fixed, and that lateral movements are negligible below the top 1-cm soil layer. The mobile dissolved ^{137}Cs activity concentration is a limited component of the total ^{137}Cs inventory (Nakanishi *et al*., 2014; Iwagami *et al*., 2017), and the uptake of ^{137}Cs by vegetation is negligible (Nishikiori *et al*., 2015a). The ^{137}Cs activity concentrations in the 0–1cm surface soil layer create uncertainty in the litter contribution rate to *TM* (*p)*. The horizontal variations in the concentration in surface soil (0–1 cm) in each of the three areas analyzed covered a range of ±60%. To assess errors related to vertical variation, the 1–2-cm and 2–3-cm concentrations were compared to the 0–1-cm concentration in each area. The concentrations at 1–2 cm and 2–3 cm were 60–90% and 35–80% of the concentration at 0–1 cm, respectively. These horizontal and vertical variations in surface soil ^{137}Cs activity concentrations resulted in approximately 8% (2–20%) uncertainty in *p* estimation. When these uncertainties were considered, the influence of litter transport on ^{137}Cs redistribution on the hillslope remained significant.

4.4 Predicted ^{137}Cs transport and spatial distribution on the forest hillslope

In this study, we found that ^{137}Cs transport with litter and sediment accounted for less than 0.5% of the ^{137}Cs inventory in 2017. We estimated a rapid decrease in litter Q_{TM} levels from

2011–2012 to 2017 due to decreased ^{137}Cs activity concentrations in the litter and organic layer, as well as vertical ^{137}Cs transport into subsurface soil during litter decomposition. If average rainfall continues, we expect Q_{TM} to decrease further and spatial changes in the ^{137}Cs inventory to stabilize, as the ^{137}Cs activity concentration in surface soil will decrease with further vertical movement of ^{137}Cs (Nakanishi *et al.*, 2015a; Kato *et al.*, 2017; Hashimoto *et al.*, 2020). However, if rainfall greatly exceeds previous rainfall levels, a large ^{137}Cs transport event may occur. In October 2019, maximum daily rainfall equivalent to the 100-year probability rainfall event was observed due to a typhoon. At that time, unexpectedly severe sediment erosion may have occurred. Consideration of the effects of heavy rainfall is essential to better predicting future ^{137}Cs movement.

Downslope accumulation of ^{137}Cs may represent a main source of ^{137}Cs cycling in plant and stream ecosystems (Koarashi et al., 2014; Murakami et al., 2014; Sakai et al., 2016) and a long-term source of dissolved and particulate ^{137}Cs output to streams (Iwagami et al., 2019; Onda et al., 2020b). Although the rate of ^{137}Cs runoff via streamflow was found to be negligible compared to the forest soil ^{137}Cs inventory (Yamashiki et al., 2014; Evrard et al., 2015), heavy rainfall can also trigger sediment transport of ^{137}Cs due to slope failure or the erosion of ^{137}Cs-contaminated soil in riparian zones. Therefore, our hillslope ^{137}Cs spatial distribution results can facilitate predictions of ^{137}Cs discharge from forested catchments.

The results of this study suggest that the spatial distribution of ^{137}Cs on the deciduous broadleaf forest hillslope in our study area is influenced by three factors: forest composition, the timing of the FDNPP accident, and high litter mobility. The FDNPP accident occurred in March, when the predominantly deciduous broadleaf trees were leafing out, which allowed high ^{137}Cs deposition directly onto the forest floor. Then, the highly mobile broadleaf litter transported ^{137}Cs throughout the study area within 1–2 years of the accident.

On the slopes of conifer-dominated forests, less ^{137}Cs transport and a more homogeneous spatial distribution of ^{137}Cs are expected, partly due to the limited mobility of coniferous needle litter compared to broadleaf litter (Hart et al., 2013), and partly because conifers trapped more ^{137}Cs in the canopy in March 2011, decreasing direct deposition onto the forest floor and subsequently delaying transfer to the forest floor via throughfall (Kato et al., 2017; Onda et al., 2020b).

The spatial distribution of the ^{137}Cs inventory on forest hillslopes remains poorly understood; further studies should collect ^{137}Cs transport data to assess the impacts of extreme rainfall events on forest hillslopes hosting various tree species and occupying diverse topographies to evaluate the broader ^{137}Cs dynamics of forest ecosystems.

5. Conclusion

This study investigated the spatial distribution of the ^{137}Cs inventory on a steep hillslope covered with broadleaf forest in Fukushima, Japan, and the impacts of ^{137}Cs transport via sediment and litter movement on the spatial distribution of the ^{137}Cs inventory. We found that the bottom slope area had a larger ^{137}Cs inventory than the upper slope on this forested hillslope covered with deciduous trees in 2017. ^{137}Cs transport along the slope surface with litter and sediment from 2016 to March 2018 accounted for less than 0.5% of the initial ^{137}Cs inventory.

The mass balance model results suggest that the spatial distribution of the ^{137}Cs inventory on the forested hillslope resulted from the movement of litter with high ^{137}Cs activity concentrations in the years following the Fukushima Daiichi Nuclear Power Plant accident. Previous studies have focused primarily on ^{137}Cs transport due to sediment movement and showed that the effect on the ^{137}Cs inventory was negligible. By contrast, this study suggests that initial litter movement may have had a significant effect on the spatial distribution of the ^{137}Cs inventory. In the future, the spatial distribution of the ^{137}Cs inventory on the hillslope will likely stabilize, if the average level of precipitation is maintained. However, heavy rainfall may cause downward movement of soil and litter and erosion in the riparian area, resulting in ^{137}Cs transport downslope and runoff downstream. Therefore, the dynamics of sediment and litter during extreme rainfall events require elucidation.

References

Abe, T., Sakamoto, T., Tanaka, H., Kabeya, N., Nobuhiro, T., Hagino, H. (2009) Estimation of downslope leaf-litter transport on a forest floor using artificial leaves. J. Jpn. For. Soc. 91, 104–110.

Atarashi-Ando, M., Koarashi, J., Takeuchi, E., Tsuduki, K., Nishimura, S., Matsunaga, T. (2015) Catchment-scale distribution of radiocesium air dose rate in a mountainuous deciduous forest and its relation to topography. Journal of Environmental Radioactivity, 147, 1-7.

Benfield, E. F. (1997) Comparison of litterfall input to streams. Journal of the North American Benthological Society 16:104–108.

Endo, I., Ohte, N., Iseda, K., Tanoi, K., Hirose, A., Kobayashi, N. I., Murakami, M., Tokuchi, N., Ohashi, M. (2015) Estimation of radioactive 137-cesium transportation by litterfall, stemflow and throughfall in the forests of Fukushima. Journal of Environmental Radioactivity, 149, 176-185.

Endo, I., Ohashi, M., Tanoi, K., Kobayashi, N.I., Hirose, A., Ohte, N. (2018) Studying 137Cs dynamics during litter decomposition in three forest types in the vicinity of Fukushima Dai-ichi Nuclear Power Plant, Journal of Forest Research, 23:2, 85-90, DOI:

10.1080/13416979.2018.1460189

Evrard, O., Laceby, J.P., Lepage, H., Onda, Y., Cerdan, O., Ayarault, S. (2015) Radiocesium transport from hillslopes to the Pacific Ocean after the Fukushima Nuclear Power Plant accident: A review. Journal of Environmental Radioactivity, 148, 92-110.

Fisher, S.A. (1977) Organic matter processing by a stream segment ecosystem: Fort River, Massachusetts, U.S.A. Internationale Revue der gesamten Hydrobiologie 62: 701–727.

France, R. L. (1995) Empirically estimating the lateral transport of riparian leaf litter to lakes. Freshwater Biology 34, 495–499.

Funada, S., Yoshimura, C., Ishidaira, H., Takeuchi, K. (2007) Observation of leaf-litter dynamics by using individual identification technique of IC tag. The Journal of Japan Society of Civil Engineers, 51, 1159-1164.

Ghahramani, A., Ishikawa, Y., Gomi, T. (2011) Slope length effect on sediment and organic litter transport on a steep forested hillslope: upscaling from plot to hillslope scale. Hydrological Research Letters 5, 16–20.

Hart, S. K., Hibbs, D.E., Perakis, S.S. (2013) Riparial litter inputs to streams in the central Oregon Coast Range. Freshwater Science, 32, 343-358.

Hashimoto, S., Ugawa, S., Nanko, K., Shichi, K. (2012) The total amounts of radioactively contaminated materials in forests in Fukushima. Scientific Reports. 2, 416. http://dx.doi.org/10.1038/srep00416.

Hashimoto, S., Imamura, N., Kaneko, S., Komatsu, M., Matsuura, T., Nishina, K., Ohashi, S. (2020) New predictions of ^{137}Cs dynamics in forests after the Fukushima nuclear accident. Scientific Reports, 10:29. https://doi.org/10.1038/s41598-019-56800-5.

Imaizumi, F., Nishii, R., Ueno, K., Kurobe, K. (2019) Forest harvesting impacts on microclimate conditions and sediment transport activities in a humid periglacial environment. Hydrol. Earth Syst. Sci., 23, 155–170.

Imamura, N., Komatsu, M., Ohashi, S., Hashimoto, S., Kajimoto, T., Kaneko, S., Tkano, T., (2017) Temporal changes in the radiocesium distribution in forests over the five years after the Fukushima Daiichi Nuclear Power Plant accident. Scientific Reports, 7: 8179.

Iwagami, S., Onda, Y., Tsujimura, M., Hada, M., Pun, I. (2017) Vertical distribution and temporal dynamics of dissolved ^{137}Cs concentrations in soil water after the Fukushima Dai-ichi Nuclear Power Plant accident. Environmental Pollution, 230, 1090-1098.

Iwagami, S., Onda, Y., Sakashita, W., Tsujimura, M., Satou, Y., Konuma. R., Nishino, M., Abe, Y. (2019) Six-year monitoring study of ^{137}Cs discharge from headwater catchments after the Fukushima Dai-ichi Nuclear Power Plant accident. Journal of Environmental Radioactivity, 210:106001.

Japanese Forestry Agency, March 31, (2012) Prefecture Proportion of Forested Land and Artificial Forest Land. http://www.rinya.maff.go.jp/j/keikaku/genkyou/h24/1.html

Japan Meteorological Agency. Past weather Data of Iitate Between 1980 to 2010.

http://www.data.jma.go.jp/gmd/risk/obsdl/index.php#!table (accessed in 2019.2.22. In Japanese).

Jones, J. A. (1987) The effects of soil piping on contributing areas and erosion patterns. Earth Surface Processes and Landforms, 12: 229– 248.

Kashihara, M. (2014) Changes in spatial distribution of radiocesium deposited from the nuclear power plant accident with surface soil movement in a forest of Fukushima. Graduation thesis of University of Tsukuba, Tsukuba, Japan (in Japanese)

Kato, H., Onda, Y., Hisadome, K., Loffredo, N., Kawamori, A. (2017) Temporal changes in radiocesium deposition in various forest stands following the Fukushima Dai-ichi Nuclear Power Plant accident. Journal of Environmental Radioactivity, 166, 449-457.

Kato, H., Onda, Y., Saidin, Z.H. (2019a). Six-year monitoring study of radiocesium transfer in forest environments following the Fukushima nuclear power plant accident. Journal of Environmental Radioactivity, 210, 105817, https://doi.org/10.1016/j.jenvrad.2018.09.015.

Kato, H., Onda, Y., Gao, X., Sanada, Y. & Saito, K. (2019b) Reconstruction of a Fukushima accident-derived radiocesium fallout map for environmental transfer studies. Journal of Environmental Radioactivity, 210, 105996.

Koarashi, J., Moriya, K., Atarashi-Ando, M., Matsunaga, T., Fujita, H., Nagaoka, M. (2012) Retention of potentially mobile radiocesium in forest surface soils affected by the Fukushima nuclear accident. Scientific Reports, 2: 1005 | Doi: 10.1038/srep01005.

Koarashi, J., Atarashi-Ando, M., Takeuchi, E., Nishimura, S. (2014) Topographic heterogeneity effect on the accumulation of Fukushima-derived radiocesium on forest floor driven by biologically mediated processes. Scientific Reports, 4: 6853 | DOI:10.1038/srep06853.

Konoplev, A., V. Golosov, V., Laptev, G., Nanba, K., Onda, Y., Takase, T., Wakiyama, Y., Yoshimura, K. (2016) Behavior of accidentally released radiocesium in soil-water environment: Looking at Fukushima from a Chernobyl perspective. Journal of Environmental Radioactivity, 151: 568-578.

Larsen, M. C., Torres-Sanchez, A. J., Concepcion, I. M. (1999) Slopewash, surface runoff and fine-litter transport in forest and landslide scars in humid tropical steeplands, Luquillo Experimental Forest, Puerto Rico. Earth Surf. Process. Landforms 24, 481-502.

Miura, S., Hirai, K., Yamada, T. (2002) Transport rates of surface materials on steep forested slopes induced by raindrop splash erosion, Journal of Forest Research, 7:4, 201-211, DOI: 10.1007/BF02763133.

Miura, S., Yoshinaga, S., Yamada, T. (2003) Protective effect of floor cover against soil erosion on steep slopes forested with *Chamaecyparis obtusa* (hinoki) and other species. Journal of Forest Research, 8(1), 27-35.

Miura, S., Ugawa, S., Yoshinaga, S., Yamada, T., Hirai, K. (2015) Floor Cover Percentage Determines Splash Erosion in Forests. Soil Science Society of America Journal 79, 1782. https://doi.org/10.2136/sssaj2015.05.0171.

Murakami, M., Ohte, N., Suzuki, T., Ishii, N., Igarashi, Y., Tanoi, K. (2014) Biological proliferation of cesium-137 through the detrital food chain in a forest ecosystem in Japan. Scientific Reports, 4: 3599 | DOI: 10.1038/srep03599.

Murakami, M., Miyata, T., Kobayashi, N., Tanoi, K., Ishii, N., Ohte, N. (2019) The Spatial Distribution of Radiocesium Over a Four-Year Period in a Forest Ecosystem in North Fukushima After the Nuclear Power Station Accident. Agricultural Implications of the Fukushima Nuclear Accident (III) (eds Nakanishi, T. M. O`Brien, M. & Tanoi, K.), Springer, Singapore, 141-152.

Muto, K., Atarashi-Andoh, M., Matsunaga, T., Koarashi, J. (2019) Characterizing vertical migration of 137Cs in organic layer and mineral soil in Japanese forests: Four-year observation and model analysis. Journal of Environmental Radioactivity, 208-209, 106040. https://doi.org/10.1016/j.jenvrad.2019.106040

Nakanishi, T., Matsunaga, T., Koarashi, J. & Atarashi-Andoh, M. (2014) ^{137}Cs vertical migration in a deciduous forest soil following the Fukushima Dai-ichi Nuclear Power Plant accident. J. Environ. Radioact. 128, 9–14.

Nakanishi, T., Funaki, H., Sakuma, K. (2021) Factors affecting ^{137}Cs concentrations in river water under base-flow conditions near the Fukushima Dai-ichi Nuclear Power Plant. Journal of Radioanalytical and Nuclear Chemistry, https://doi.org/10.1007/s10967-021-07735-7.

Nanko, K., Mizugaki, S., Onda, Y. (2008) Estimation of soil splash detachment rates on the forest floor of an unmanaged Japanese cypress plantation based on field measurements of throughfall drop sizes and velocities. Catena, 72, 348-361, 10.1016/j.catena.2007.07.002.

Niizato, T., Abe, H., Mitachi, K., Sasaki, Y., Ishii, Y., Watanabe, T. (2016) Input and output budgets of radiocesium concerning the forest floor in the mountain forest of Fukushima released from the TEPCO's Fukushima Dai-ichi power plant accident. Journal of Environmental Radioactivity, 161,11-21.

Nishikiori, T.,Watanabe, M., Koshikawa, M.K., Takamatsu, T., Ishii, Y., Ito, S., Takenaka, A., Watanabe, K., Hayashi, S. (2015a) Uptake and translocation of radiocesium in cedar leaves following the Fukushima nuclear accident. Sci. Total Environ. 502, 611–616. https://doi.org/10.1016/j.scitotenv.2014.09.063.

Nishikiori, T., Ito, S., Tsuji, H., Yasutaka, T., Hayashi, S. (2015b) Influence of Forest Floor Covering on Radiocesium Wash-off Associated with Forest Soil Erosion, J. Jpn. For. Soc. 97, 63-69.

Ohte, N., Murakami, M., Endo, I., Ohashi, M., Iseda, K., Suzuki, T., Oda, T., Hotta, N., Tanoi, K., Kobayashi, N.I., Ishii, N. (2016) Ecosystem monitoring of radiocesium redistribution dynamics in a forested catchment in Fukushima after the nuclear power plant accident in March 2011. Agricultural Implications of the Fukushima Nuclear Accident (eds Nakanishi, T. M. & Tanoi, K.), Springer, Tokyo, 175-188.

Onda, Y., Taniguchi K, Yoshimura K, Kato H, Takahashi J, Wakiyama Y, Coppin F, Smith H.

(2020a) Radionuclides from the Fukushima Daiichi Nuclear Power Plant in terrestrial systems. Nature Reviews Earth and Environment, 1:644–660. https://doi.org/10.1038/s43017-020-0099-x

Onda, Y., Hayashi, S., Nagao, S., Ishii, Y., Tsuji, H., Taniguchi, K., Nishina, K., Suzuki, K., Watanabe, S., Prohl, G., Boyer, P., Laurent, G. (2020b) Catchments and Rivers Chapter 6. IAEA-TECDOC-1927, 179-227.

Orndorff, K. A., Lang, G. E. (1981) Leaf Litter Redistribution in a West Virginia Hardwood Forest. Journal of Ecology, 69(1), 225–235. https://doi.org/10.2307/2259827.

Plamboeck, A.H., Nylen, T., Grip, H. (2000) Uptake of cations under two different water regimes in a boreal Scots pine forest. Sci. Total Environ. 256, 175–183. https://doi.org/10.1016/S0048-9697(00)00483-6.

Pumpanen, J., Ohashi, M., Endo, I., Hari, P., Bäck, J., Kulmala, M., Ohte, N. (2016) 137Cs distributions in soil and trees in forest ecosystems after the radioactive fallout–Comparison study between southern Finland and Fukushima, Japan. Journal of Environmental Radioactivity, 161: 73-81. https://doi.org/10.1016/j.jenvrad.2016.04.024

Sala, M. (1988) Slope runoff and sediment production in two Mediterranean mountain enviroments. CATENA Suppl., 12:13–29.

Sakai, M., Gomi, T., Negishi, J. N., Iwamoto, A., Okada, K. (2016) Different cesium-137 transfers to forest and stream ecosystems. Environmental Pollution, 209, 46-52.

Schaub, M., Konz, N., Meusburger, K., Alewell, C. (2010) Application of in-situ measurement to determine 137Cs in the Swiss Alps. Journal of Environmental Radioactivity. 101, 369-376.

Shcheglov, A.I., Tsvetnova, O.B., Klyashtorin, A.L. (2001) Biogeochemical migration of technogenic radionuclides in forest ecosystems. Nauka Moscow, -235p.

Takahashi, J., Tamura, K., Suda, T., Matsumura, R., Onda, Y. (2015) Vertical distribution and temporal changes of ^{137}Cs in soil profiles under various land uses after the Fukushima Dai-ichi Nuclear Power Plant accident. Journal of Environmental Radioactivity, 139, 351-361.

Takahashi, J., Onda, Y., Hihara, D., Tamura, K. (2018) Six-year monitoring of the vertical distribution of radiocesium in three forest soils after the Fukushima Dai-ichi Nuclear Power Plant accident. Journal of Environmental Radioactivity, 192, 172-180.

Taniguchi, K., Onda, Y., Smith, H.G., Blake, W., Yoshimura, K., Yamashiki, Y., Kuramoto, T., Saito, K. (2019) Transport and redistribution of radiocesium in Fukushima fallout through rivers. Environmental Science and Technology, 53, 12339-12347.

Tsukamoto, J. (1991) Downhill movement of litter and its implication for ecological studies in three types of forest in Japan. Ecological Research 6, 333–345. https://doi.org/10.1007/BF02347132

Uchida T, Kosugi K, Mizuyama T. (2001) Effects of pipeflow on hydrological process and its relation to landslide: a review of pipeflow studies in forested headwater catchments. Hydrological Processes 15: 2151– 2174. DOI: 10.1002/hyp.281.

Wakahara, T., Ishikawa, Y., Shiraki, K., Toda, H., Miya, T., Kataoka, F., Suzuki, M., Uchiyama, Y. (2008) Seasonal changes in the amount of litter layer and soil erosion in the forest floor: an impoverished understory by deer impact an Doudaira, Tanzawa Mountains. J Jpn For Soc. 90:378–385 (in Japanese with English abstract).

Wakiyama, Y., Onda, Y., Yoshimura, K., Igarashi, Y., Kato, H. (2019) Land use types control solid wash-off rate and entrainment coefficient of Fukushima-derived ^{137}Cs, and their time dependence. Journal of Environmental Radioactivity, 210, 105990.

Yamashiki Y, Onda, Y., Smith, H.G.,.Blake, W.H., Wakahara, T., Tachikawa, Y., Igarashi, Y., matsuura, Y., Yoshimura, K. (2014) Initial flux of sediment-associated radiocesium to the ocean from the largest river impacted by Fukushima Daiichi Nuclear Power Plant. Scientific reports |4:3714|. DOI:10.1038/srep03714: 1-7

Yoschenko, V., Takase, S., Hinton, T.G., Nanba, K., Onda, Y., Alexei Konoplev, A., Goto, A., Yokoyama, A., Keitoku, K. (2018) Radioactive and stable cesium isotope distributions and dynamics in Japanese cedar forests. Journal of Environmental Radioactivity, 186, 34-44.

Yoshimura, K., Onda, Y., Kato, H. (2015) Evaluation of radiocaesium wash-off by soil erosion from various land use using USLE plots. Journal of Environmental Radioactivity, 139, 362-369.

Figure captions

Figure 1. (a) Map of initial ^{137}Cs deposition and the location of the study site (from Endo et al., 2015), (b) topographic map of subplots on the slope, and (c) longitudinal sectional view of the slope subplots. Black dots in panel (b) indicate soil sampling locations, and red dots in panels (b) and (c) indicate sediment trap locations (ST1, ST2, and ST3). In panel (c), the numbers 1 to 6 indicate subplots, and black dots indicate the average elevation and distance of each soil sampling location in each subplot.

Figure 2. Photographs of the experimental hillslope (a), litter trap (b), and sediment trap (c), and diagram of the sediment trap structure (d).

Figure 3. Schematic of the model. The box with a dashed outline represents the ground litter layer, and the two boxes with solid outlines below the litter layer represent the surface soil and subsurface soil. The ^{137}Cs inventories in each layer are S_{litter}, S_{soil}, and $S_{subsoil}$, respectively, and arrows indicate the amounts of ^{137}Cs moved (Q).

Figure 4. Mean ^{137}Cs inventory profiles in the soil layers of Subplots 1 to 6 in November 2017. Bars indicate standard deviations.

Figure 5. Relationship between the mean ^{137}Cs inventory in each subplot and distance from the stream channel. Bars indicate standard deviations.

Figure 6. ^{137}Cs activity concentrations in leaf litter (C_{litter}), transported material (C_{TM}), and 1-cm surface soil layer (C_{soil}). Error bars indicate standard errors.

Figure 7. Temporal variations in the (a) monthly rainfall, (b) rainfall erosivity factor (R), (c) daily mean material transport rate (TM), (d) daily mean ^{137}Cs transport rate (Q_{TM}), and (e) mean ^{137}Cs activity concentration in transported material (C_{TM}) from October 2016 to March 2018.

Figure 8. Calculated ^{137}Cs inventory changes from 2011 to 2018 in the (a) ridge (S_{ridge}), (b) slope (S_{slope}), and (c) riparian (S_{rip}) areas due to lateral material transport with rates of attachment of initially deposited ^{137}Cs to the litter of 100% (○), 50% (△), and 0% (●). Diamonds (◆) indicate the observed mean ^{137}Cs inventory for each area in 2017. Error bars indicate standard errors.

Tables

Table 1. List of input parameters for the mass balance model and their abbreviations.

Parameters (Abbreviation)	Description	Unit	Value
α	Initial ^{137}Cs adherence rate to litter	-	0 - 1
β	Leaf decomposition rate	1/year	0.7
γ	vertical ^{137}Cs transport rate in the soil layer	-	0.23-0.25
p	Litter contribution rate to transport material	-	0.96
q	the contribution rate of litter transport to ^{137}Cs transport	-	
D	Soil density	Mg/m^3	0.194
Sc	Entrainment coefficient	m^2/kg	
R	Rainfall erosivity factor	MJ mm/ha h	
S	Slope steepness factor	-	
K	Soil erosivity factor	-	0.02
LF	Annual litterfall amount	kg/m^2/year	
TM	Material transport rate	kg/m^2/year	
LG	leaf litter amount on the ground	kg/m^2/year	
C_{LF}	^{137}Cs activity concentration in the litterfall	kBq/kg	
C_{soil}	^{137}Cs activity concentration in the surface soil	kBq/kg	
C_{litter}	^{137}Cs activity concentration in the ground leaf litter	kBq/kg	
C_{TM}	^{137}Cs activity concentration in the transported material	kBq/kg	
Q_{LF}	Annual ^{137}Cs input by litterfall	kBq/m^2/year	
Q_{TM}	Annual transported ^{137}Cs on the hillslope	kBq/m^2/year	
Q_D	Vertical ^{137}Cs transfer from the litter layer to the soil layer	kBq/m^2/year	
Qv	Vertical ^{137}Cs transfer from the surface soil layer to the subsurface soil layer	kBq/m^2/year	
Q_{Up}	^{137}Cs uptake by plants	kBq/m^2/year	
$S_{initial}$	Initial ^{137}Cs deposition at the study site	kBq/m^2	
S_{rip}	^{137}Cs inventory of the riparian area	kBq/m^2	
S_{slope}	^{137}Cs inventory of the slope area	kBq/m^2	
S_{ridge}	^{137}Cs inventory of the ridge area	kBq/m^2	
S_{litter}	^{137}Cs inventory of the litter layer	kBq/m^2	
S_{soil}	^{137}Cs inventory of the surface soil layer	kBq/m^2	
$S_{subsoil}$	^{137}Cs inventory of the subsurface soil layer	kBq/m^2	

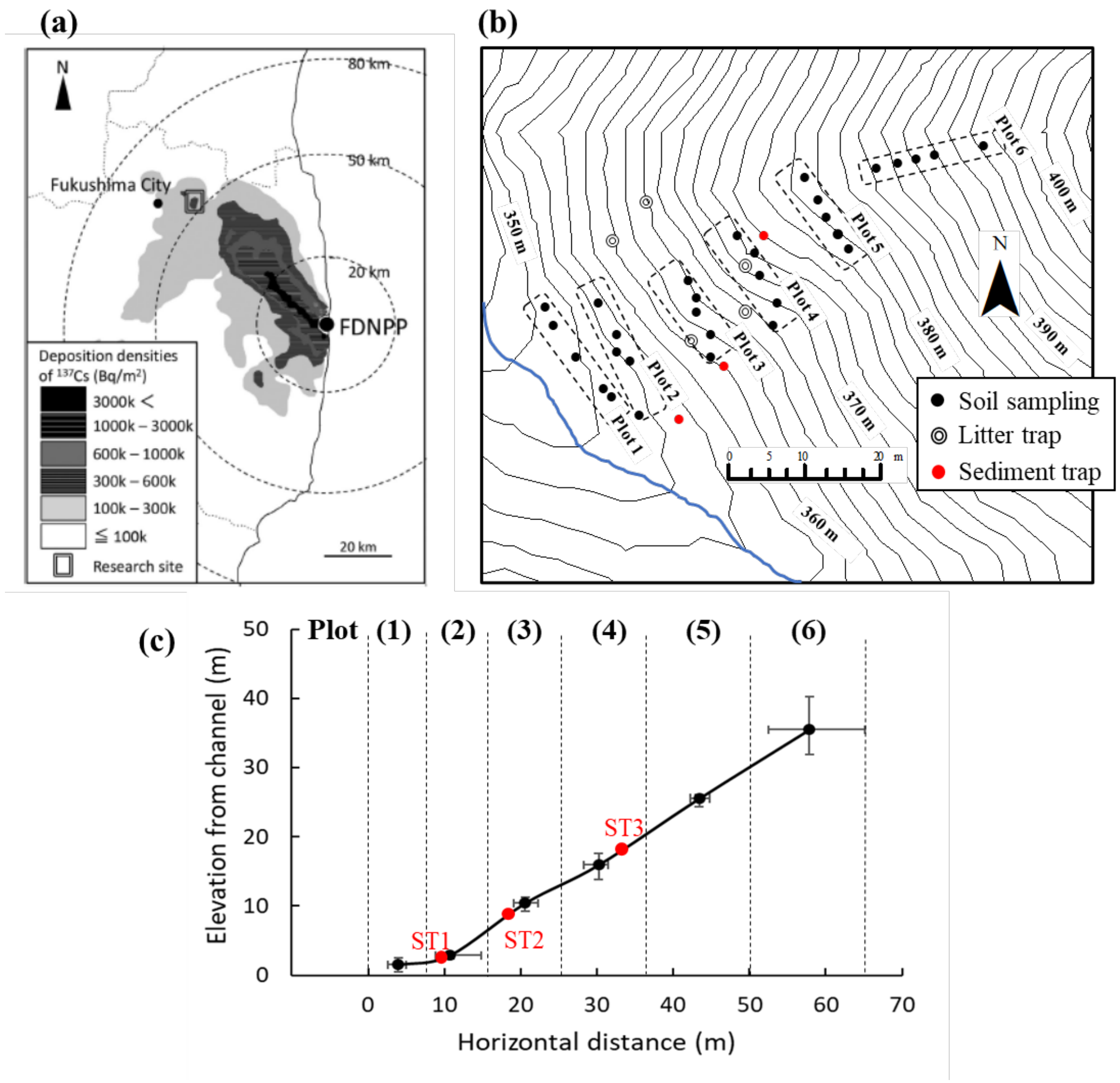
(a)
N
80 km
50 km
20 km
Fukushima City
FDNPP
Deposition densities of ¹³⁷Cs (Bq/m²)
3000k <
1000k – 3000k
600k – 1000k
300k – 600k
100k – 300k
≦ 100k
Research site
20 km
(b)
Plot 1
Plot 2
Plot 3
Plot 4
Plot 5
Plot 6
350 m
360 m
370 m
380 m
390 m
400 m
N
0 5 10 20 m
Soil sampling
Litter trap
Sediment trap
(c)
Plot (1) (2) (3) (4) (5) (6)
ST1
ST2
ST3
Elevation from channel (m)
Horizontal distance (m)
0 10 20 30 40 50
0 10 20 30 40 50 60 70

Figure 1

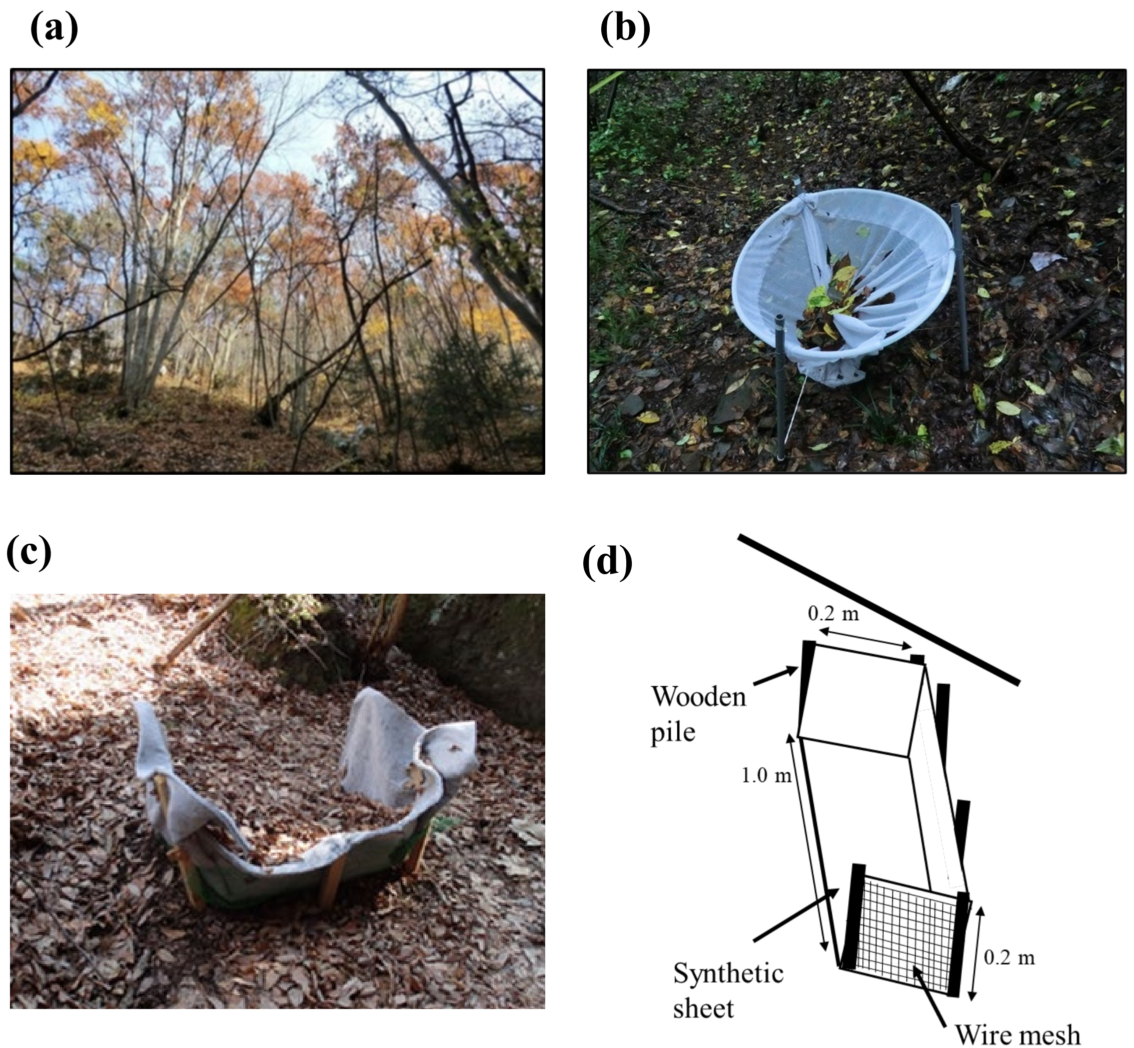

Figure 2

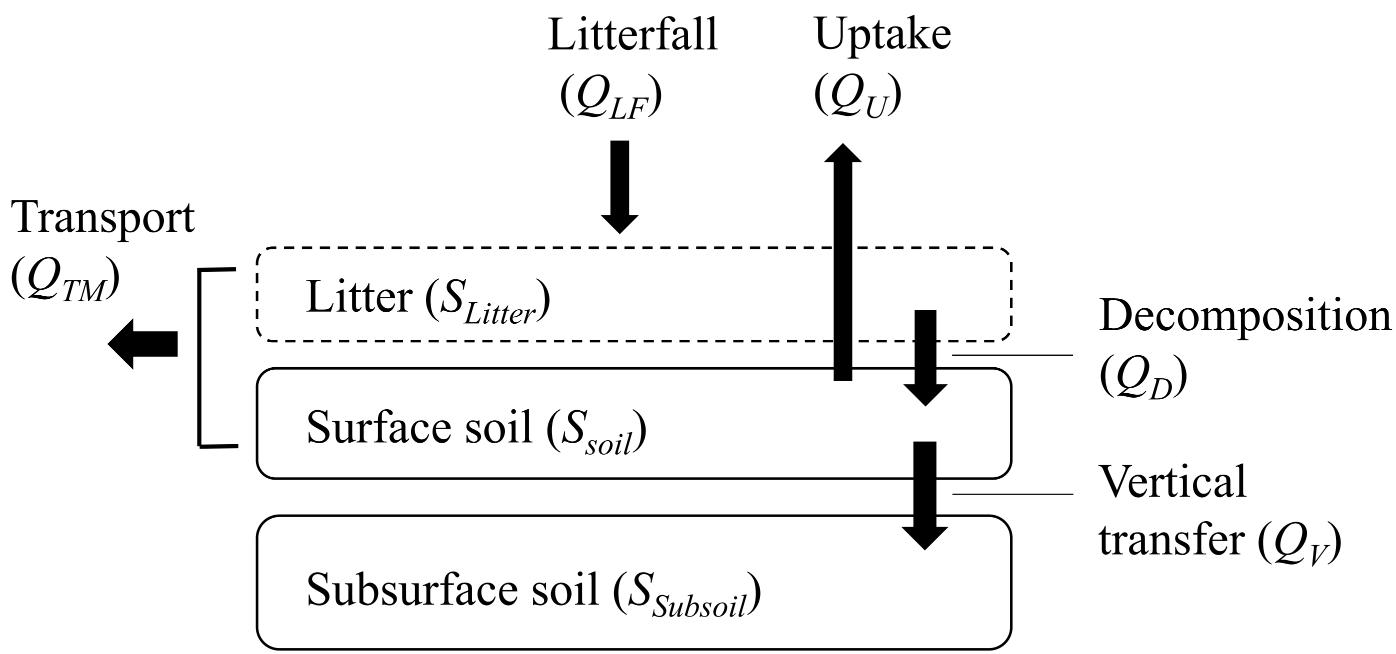
Litterfall
(Q_{LF})
Uptake
(Q_U)
Transport
(Q_{TM})
Litter (S_{Litter})
Decomposition
(Q_D)
Surface soil (S_{soil})
Vertical
transfer (Q_V)
Subsurface soil ($S_{Subsoil}$)

Figure 3

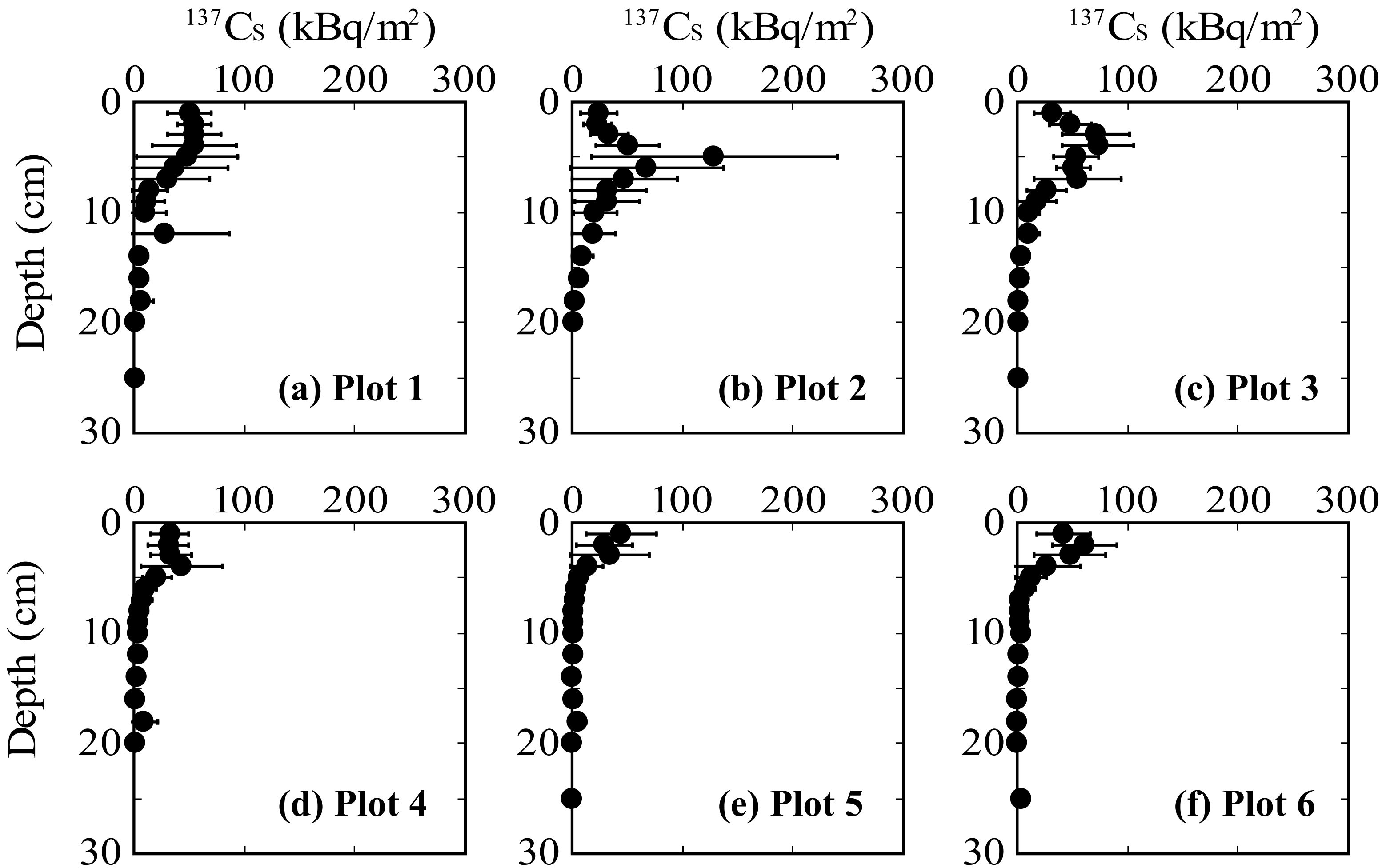
^{137}Cs (kBq/m^2)
^{137}Cs (kBq/m^2)
^{137}Cs (kBq/m^2)
0
100
200
300
0
10
20
30
Depth (cm)
(a) Plot 1
(b) Plot 2
(c) Plot 3
(d) Plot 4
(e) Plot 5
(f) Plot 6

Figure 4

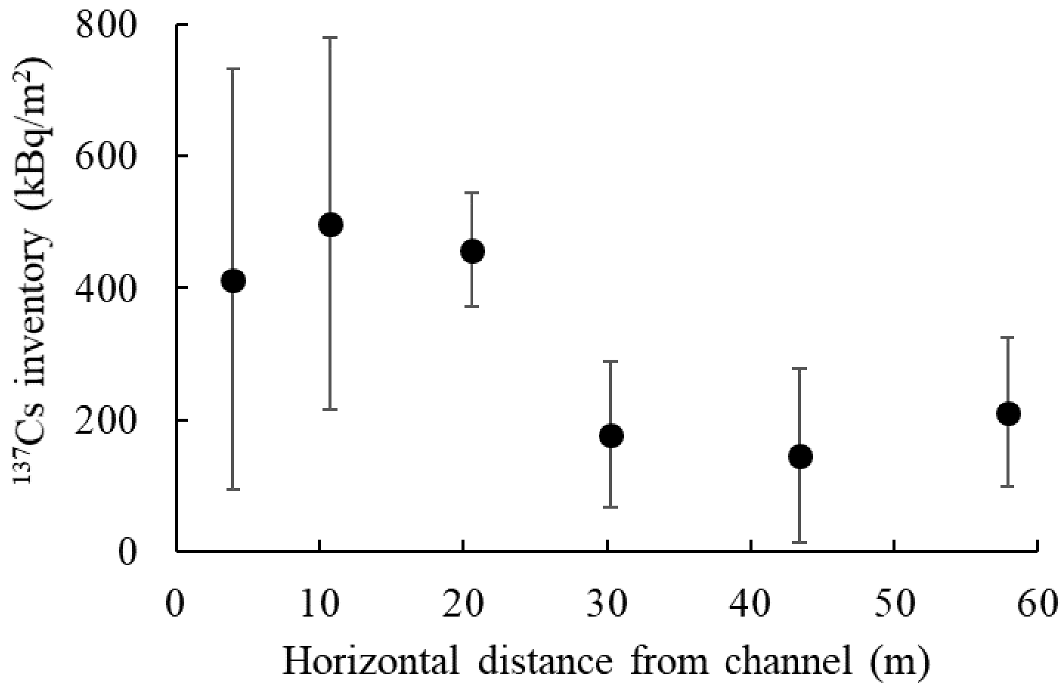

800
600
400
200
0
^{137}Cs inventory (kBq/m^2)
0
10
20
30
40
50
60
Horizontal distance from channel (m)

Figure 5

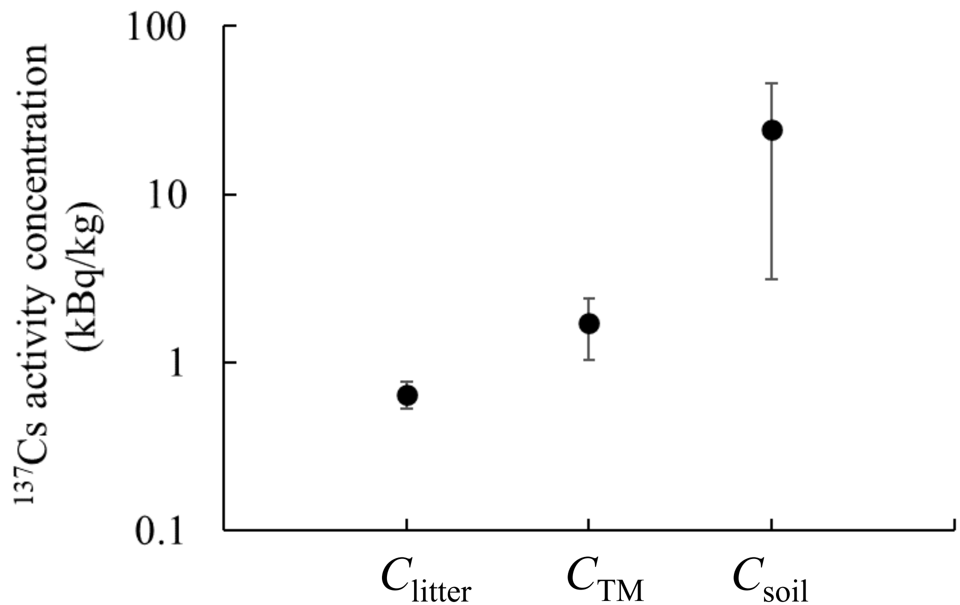

100
10
1
0.1
^{137}Cs activity concentration (kBq/kg)
C_{litter}
C_{TM}
C_{soil}

Figure 6

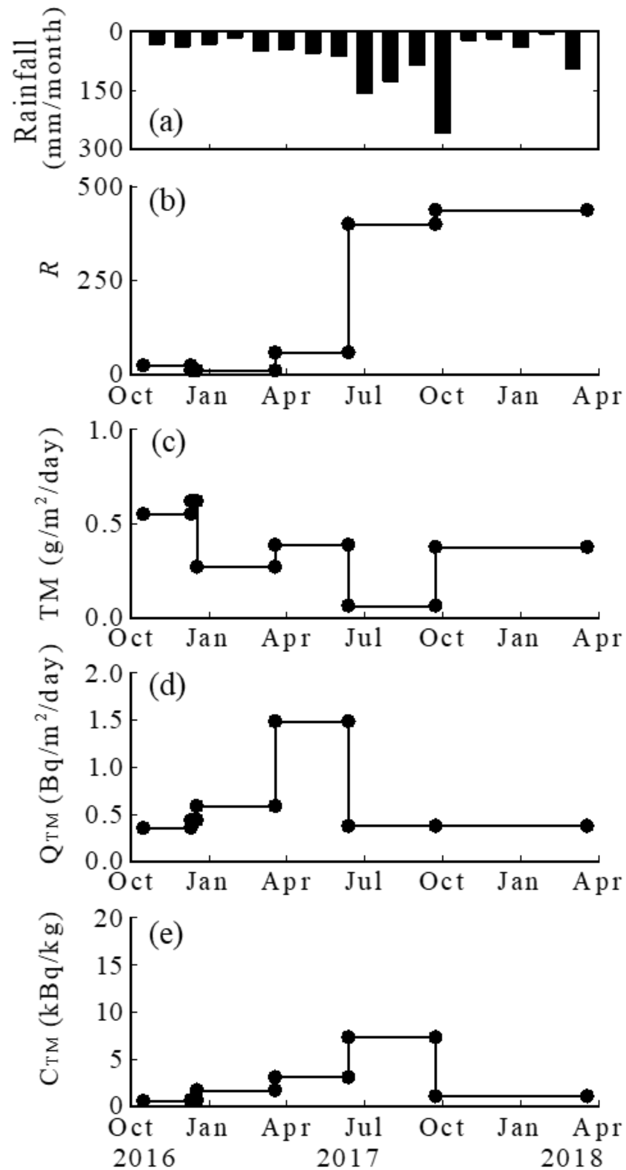
Rainfall (mm/month)
0
150
300
(a)
500
250
0
R
(b)
Oct
Jan
Apr
Jul
Oct
Jan
Apr
1.0
0.5
0.0
TM (g/m²/day)
(c)
Oct
Jan
Apr
Jul
Oct
Jan
Apr
2.0
1.5
1.0
0.5
0.0
QTM (Bq/m²/day)
(d)
Oct
Jan
Apr
Jul
Oct
Jan
Apr
20
15
10
5
0
CTM (kBq/kg)
(e)
Oct
Jan
Apr
Jul
Oct
Jan
Apr
2016
2017
2018

Figure 7

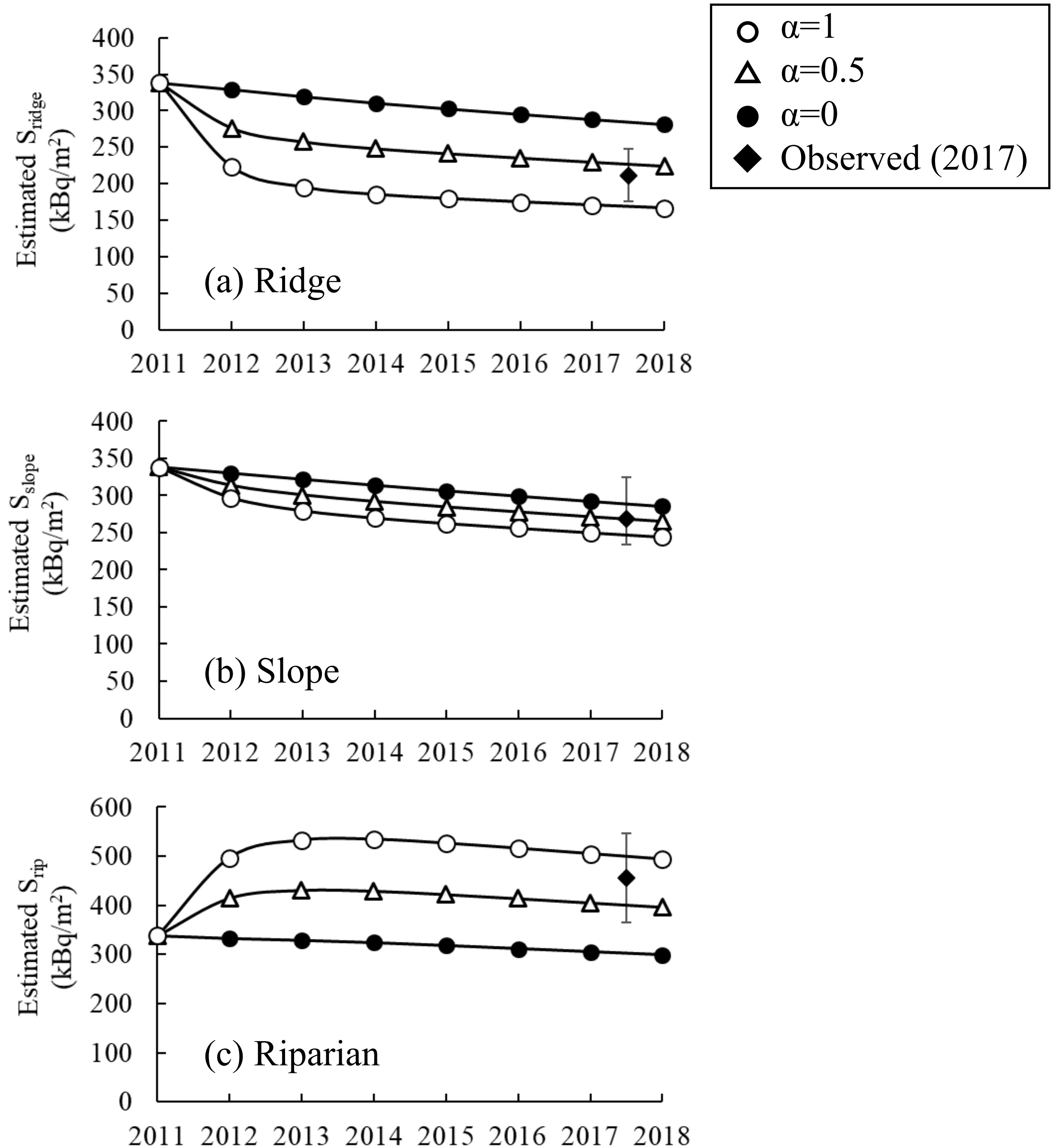
α=1
α=0.5
α=0
Observed (2017)
Estimated S_{ridge} (kBq/m^2)
(a) Ridge
Estimated S_{slope} (kBq/m^2)
(b) Slope
Estimated S_{rip} (kBq/m^2)
(c) Riparian
2011 2012 2013 2014 2015 2016 2017 2018

Figure 8

Supplementary material

Redistribution of the soil ^{137}Cs inventory through litter and sediment transport on a hillslope covered by deciduous forest in Fukushima, Japan

Authors

Tomoki Oda[1, 2], Norifumi Hotta[2], Satoru, Miura[1], Izuki Endo[3], Keitaro Tanoi[2], Chris S. Renschler[4], Nobuhito Ohte[5]

1. Department of Disaster Prevention, Meteorology and Hydrology, Forestry and Forest Products Research Institute, Ibaraki 305-8687, Japan

2. Graduate School of Agricultural and Life Sciences, The University of Tokyo, 1-1-1 Yayoi, Bunkyo-ku, Tokyo 113-8657, Japan

3. School of Human Science and Environment, University of Hyogo, Hyogo 670-0092, Japan

4. Department of Geography, University at Buffalo, The State University of New York, 116 Wilkeson Quad, Buffalo NY 14261, USA

5. Department of Social Informatics Graduate School of Informatics, Kyoto University, Kyoto 606-8501, Japan

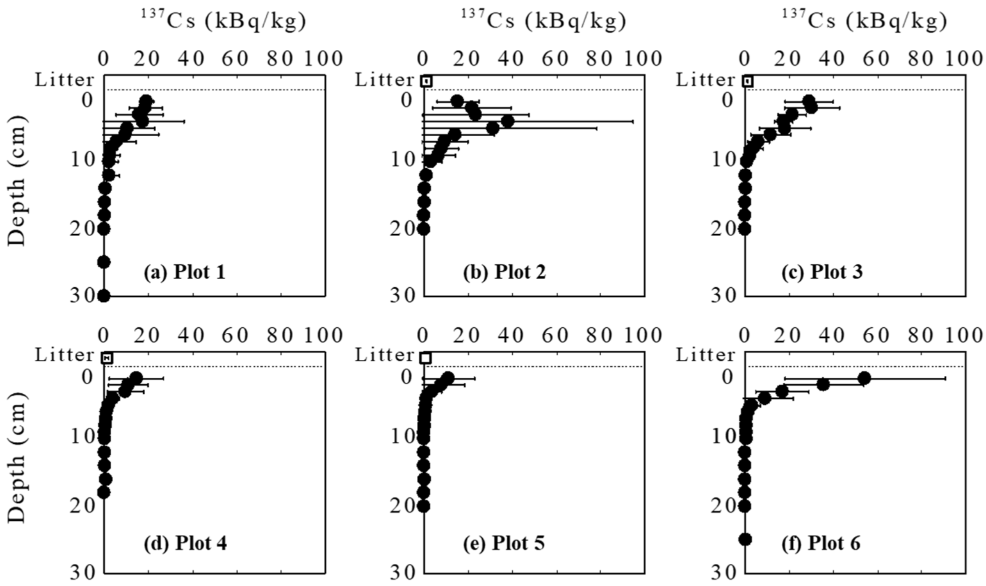

Figure S1. Mean ^{137}Cs activity concentration profiles in the soil layers (●) of Subplots 1–6 in November 2017 and mean ^{137}Cs activity concentration in the ground litter (□) in December 2016. Bars indicate standard deviations.

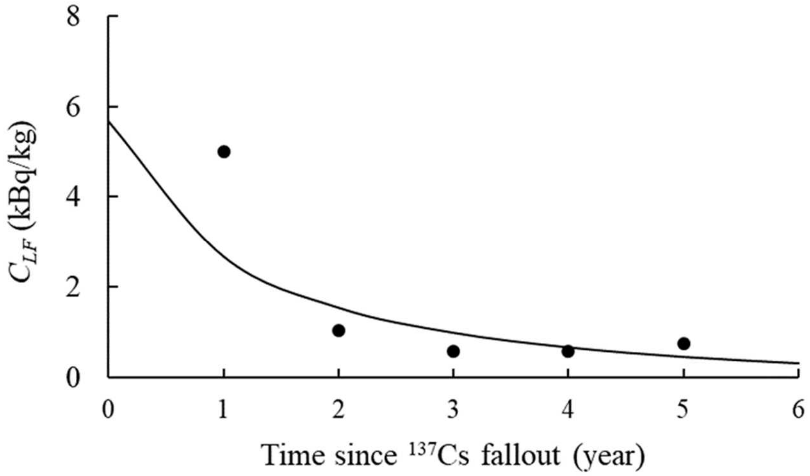

Figure S2. Changes in the average ^{137}Cs activity concentration in litterfall (C_{LF}) from the year since ^{137}Cs fallout (t). The solid line shows the fitting line by the double exponential curve ($C_{LF}(t) = 2.8e^{-0.37t} + 2.8e^{-1.38t}$).

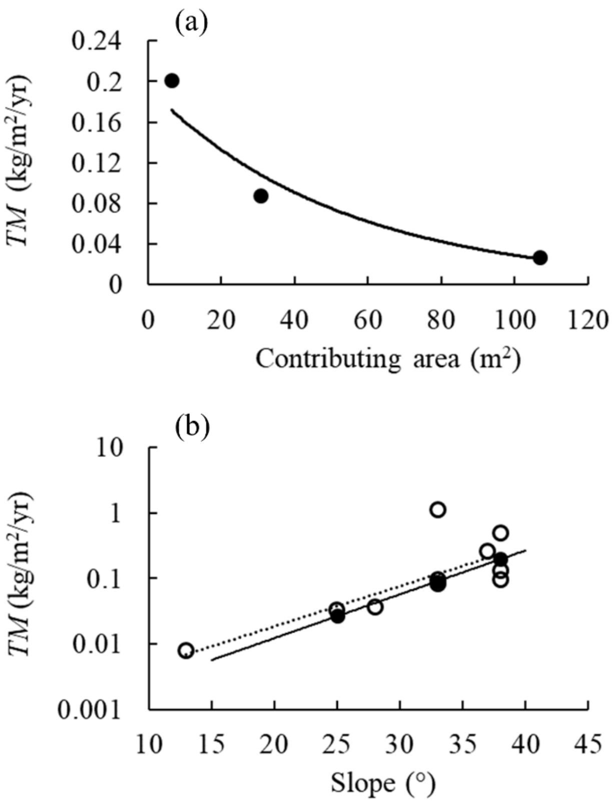

Figure S3. Relationships of the material transport rate (*TM*) with contribution area (●) (a) and slope angle (●) (b). The TM data with slope in broadleaf forests from Wakahara et al., (2008), Teramage et al., (2013), Kashihara, (2014), Nishikiori et al (2015) and Niizato et al (2016) were plotted as open circle (○). The solid lines were exponential regression lines of observed *TM* and contributing area ($y = 0.194e^{-0.019x}$, R^2=0.94) (a) and observed *TM* and slope in this study ($y = 0.0006e^{0.154x}$, R^2 = 0.99) (b). The dashed line shows exponential regression line of observed *TM* and slope in previous studies ($y= 0.0011e^{0.14x}$, R^2=0.63).

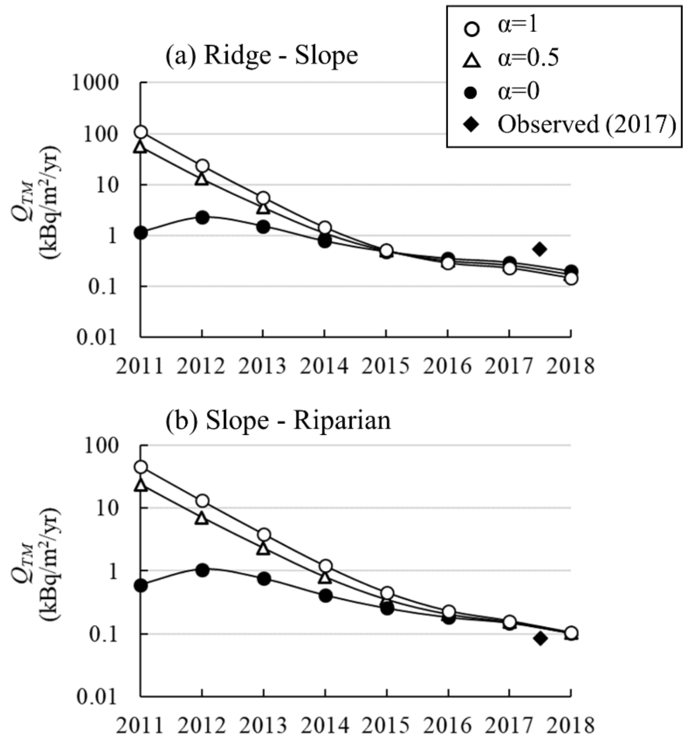

Figure S4. Calculated changes in ^{137}Cs transport from 2011 to 2018 in (a) the ridge to slope area and (b) the slope to riparian area due to lateral transport of material with rates of attachment of initially deposited ^{137}Cs to litter of 100% (○), 50% (□), and 0% (●). Diamonds (□) indicate the observed mean annual ^{137}Cs transport rates at areas around (a) ST3 and (b) ST1 and ST2.

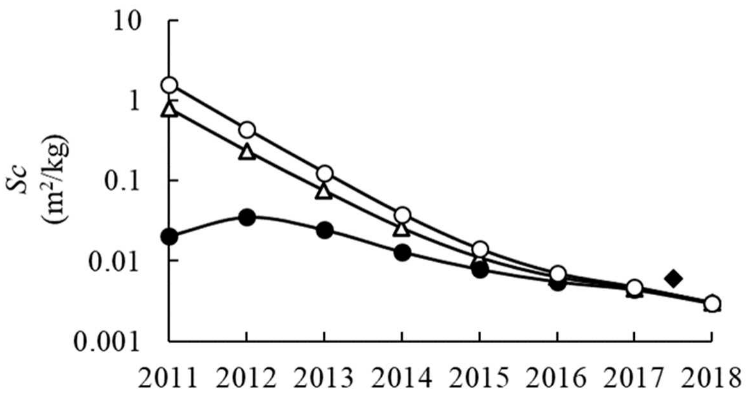

Figure S5. Calculated average entrainment coefficient (*Sc*) from 2011 to 2018 with rates of attachment of initially deposited ^{137}Cs to litter of 100% (○), 50% (△), and 0% (●). Diamonds (◆) indicate the observed *Sc* values in 2017.

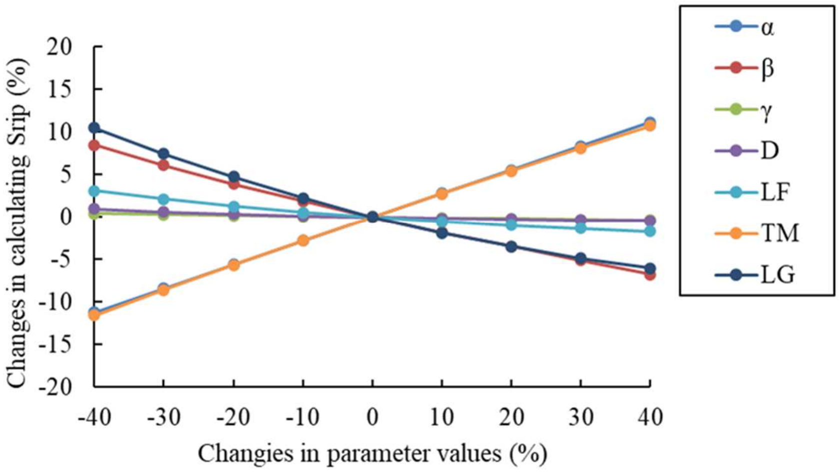

Figure S6. Results of sensitivity analysis for the ^{137}Cs mass balance model. Changes in the ^{137}Cs inventory in the riparian area with changes in the initial attachment rate (α), decomposition rate (β), vertical transfer rate to the subsurface layer (γ), soil density (D), litterfall amount (LF), material transport rate (TM), and ground litter amount (LG).

References

Kashihara, M. (2014) Changes in spatial distribution of radiocesium deposited from the nuclear power plant accident with surface soil movement in a forest of Fukushima. Graduation thesis of University of Tsukuba, Tsukuba, Japan (in Japanese)

Niizato, T., Abe, H., Mitachi, K., Sasaki, Y., Ishii, Y., Watanabe, T. (2016) Input and output budgets of radiocesium concerning the forest floor in the mountain forest of Fukushima released from the TEPCO's Fukushima Dai-ichi power plant accident. Journal of Environmental Radioactivity, 161,11-21.

Nishikiori, T., Ito, S., Tsuji, H., Yasutaka, T., Hayashi, S. (2015b) Influence of Forest Floor Covering on Radiocesium Wash-off Associated with Forest Soil Erosion, J. Jpn. For. Soc. 97, 63-69(in Japanese with English abstract).

Teramage, M., Onda, Y., Kato, H., Wakiyama, Y., Mizugaki, S., Hiramatsu, S. (2013) The relationship of soil organic carbon to 210Pbex and 137Cs during surface soil erosion in a hillslope forested environment, Geoderma 192, 59.

Wakahara, T., Ishikawa, Y., Shiraki, K., Toda, H., Miya, T., Kataoka, F., Suzuki, M., Uchiyama, Y. (2008) Seasonal changes in the amount of litter layer and soil erosion in the forest floor: an impoverished understory by deer impact an Doudaira, Tanzawa Mountains. J Jpn For Soc. 90:378–385 (in Japanese with English abstract).